Study on the Prevention of Postoperative Pleural Adhesion: Development of an Insoluble Hyaluronic Acid Membrane Using Surface Water Induction Technology

January 2019

Akiko UEMURA

Study on the Prevention of Postoperative Pleural Adhesion: Development of an Insoluble Hyaluronic Acid Membrane Using Surface Water Induction Technology

A Dissertation Submitted to

the Graduate School of Life and Environmental Sciences,

the University of Tsukuba

in Partial Fulfillment of the Requirements

for the Degree of Doctor of Philosophy in Agricultural Science

(Doctoral Program in Bioindustrial Sciences)

Akiko UEMURA

【 Contents 】

Chapter 1

General Introduction

The Needs of Effective New Membrane for Preventing Postoperative Pleural Adhesion and The Reason for Choosing Hyaluronic Acid as Material Membrane

Post-operative adhesions occur at a high rate. Organ damage such as abdominal pain, intestinal obstruction and infertility occurs after an abdominal surgery due to peritoneal adhesion (1, 2), and its harmful effects have been known widely. It is reported that this abdominal postoperative adhesion occurs not only in laparotomy, but also in an endoscopic surgery (3). On the other hand, post-thoracotomy adhesion also occurs at high rate, but its relevance to organ damage has not been well described. Although post-operative risk of damage to the heart and large vessels (4) has been reported, few reports mentioned the problems related to the quality of life of postoperative patients, and the level of general awareness of these complications is low. However, it is known as an important problem in thoracic surgery that post-thoracotomy adhesions cause serious harmful effects during re-operation of the chest. This is because adhesions of the chest wall, lungs and pericardium cause problems such as extended re-operation time, bleeding, inadequate view of the surgical field and pulmonary vascular injury (5-9).

To prevent post-abdominal operative adhesion, adhesion prevention membrane, mainly composed of carboxymethyl-cellulose, has become commercially available, and is reported to reduce post-abdominal operative adhesion effectively (10-13). Some reports also that suggest that this carboxymethyl-cellulose membrane was significantly effective in preventing adhesion in pediatric cardiac surgery (14) and rat mediastinoscopy examination (15). When it was applied to thoracic surgery. There are multiple methods using carboxymethyl-cellulose membrane for laparoscopy, including the one using (16-18) membrane cut into several small pieces to wrap around the forceps, and others with the reported efficacy of the carboxymethyl-cellulose membrane in laparoscopy (19, 20).

On the other hand, the need of preventing post-thoracotomy adhesion has been recognized so far which is regarded as one of the important factor in thoracic surgery. Many prevention methods have been studied for a long time (21-24), and all of them are still under the development stage and has not reached commercially available stage yet. Another type of post-operative adhesion prevention membrane using surface water induction technology is that is more effective than carboxymethyl-cellulose membrane, which is primarily comprised of glycerin with has a high water retention capacity, and it was reported to be used in dogs already (25). However, multiple risks of hemolysis that

may occur in the body due to glycerin have been reported (26, 27), and glycerine has a safety-related concern as an *in vivo* preparation. Therefore, it is necessary to develop a post-thoracotomy adhesion inhibitor with superior safety and efficacy using surface water induction technology, by switching the water-retentive compound to an *in vivo* absorptive substance with higher safety than that of glycerin.

Hyaluronic acid was discovered by Meyer as a vitreous component of bovine eyeball in 1934 (28) and is a type of glycosaminoglycan (29). Hyaluronic acid is distributed extensively in cartilage, skin, and joints as extracellular matrix in the body. Hyaluronic acid with high water retentivity contributes to the stability, lubricity and elasticity of tissues (30), and is a component having many physiological activities in the body. For its usefulness, hyaluronic acid is widely used as medicine including therapeutic agents for osteoarthritis such as shoulder joints (31) and knee joints (32, 33), anti-adhesion agents for post- abdominal operation (34, 35), as a filler (36, 37) in plastic surgery and cosmetic care. To fit these various applications, demand for hyaluronic acid to display more features as a medical product has been increasing. In particular, controlling its rates of degradation and absorption represents a significant challenge. This is because the material remaining in the body for the required amount of time and exhibiting its effects continuously; would result in more stable control of various

diseases. How hyaluronic acid formulations degrad, in addition to the degradation rate itself, is also an important factor. For example, does the material retain its form until just before degradation? Or does it gradually degrade from the begining? This difference would become a critical point when investigating its effect on a target disease or site.

Adjustment of properties and the degradation rate of hyaluronic acid is also performed by changing the molecular weight (38) and by using crosslinkers (39) (40). However, these methods have some issues left unsolved, especially safety of byproducts. On the other hand, my research collaborator founded the methods of treatment for hyaluronic acid using acetic anhydride (unpublished data). The method for insolubilization of hyaluronic acid, in accordance with the method described in previous reference (41). It is known that polysaccharide reacts with acid and produces an insolubles. For example, one of polysaccharides sodium alginate is used as a curative medicine to a regurgitant esophagus flame (42). Preliminary experiment was performed using this characteristic, hyaluronic acid was reacted with several acid. Good results were obtained by the reaction of acetic anhydride. Thus acetic anhydride was used for insolubilization of hyaluronic acid in this study.

Based on these findings, treatment for hyaluronic acid using acetic anhydride was

focused. The changing ratio were investigated the treatment time, insolubilization rate, and swelling ratio. In addition, the relationship between these ratio and degradable with decomposition behavior in thie study. Eventually, the present study aims to develop a new post-thoracotomy adhesion prevention membrane using insoluble hyaluronic acid as a water-retentive substance that can replace glycerin, with developmental processes consisting the following three steps. That is inspection of hyaluronic acid as advanced materials for a water-retentive substance, effect as anti-adhesive membrane and the research for the detection method of the pleural adhesion.

In Chapter 2 the properties of in hyaluronic acid required to be used as a post-operative adhesion inhibitor was verified. The post-operative adhesion inhibitor must remain in the surgical invasion sites such as incisional wound for about 7 days when adhesions are formed and must physically prevent such adhesion formation. Therefore, the hyaluronic acid preparation as a post-operative adhesion inhibitor must remain in the insertion site for a certain period of time to exhibit its effect, without being absorbed immediately after being inserted into the body. However, the factors that control the decomposition rate of hyaluronic acid are still unknown. If the unknown factors capable of controlling the decomposition rate of hyaluronic acid can be clarified, its utility value will be infinitely large. Another important factor to consider is how

many byproducts will be produced, and what kind of decomposition process will be encountered by this new hyaluronic acid preparation during its production process that utilizes the aforementioned unknown factors. Although hyaluronic acid has been reported to change its decomposition rate depending on the rise and fall of its swelling rate, the factors controlling the swelling rate itself are have not been clarified yet (43). Therefore, the following experiments were conducted in Chapter 2. First, three types of hyaluronic acid preparations were prepared with different swelling ratios and the decomposition processes unaffected by enzymes were examined. The changes during the hyaluronic acid preparation inside a simulated body fluid were measured and scored based on the swelling ratio.

In Chapter 3, using a dog open thoracotomy model, the chest post-thoracotomy adhesion prevention effect and the operability of insoluble hyaluronic acid membrane were investigated, of which decomposition process was elucidated in Chapter 2. Post-thoracotomy adhesion is a significant problem during re-operation. Although re-operation rate in thoracic surgery depends on the disease, chest re-operation is considered to be one of the common treatment options for treating metastasis or recurring malignant tumor (44-46). Re-operation rate in aortic valve replacement and coronary artery bypass surgery is 10% to 20% (46), and multiple operations are

common for children with congenital heart disease (47, 48). In recent years, VATS (Video-Assisted Thoracic Surgery) using a thoracoscope has been developed and is generally recognized as a minimally invasive treatment. The application of VATS on various diseases mainly in respiratory surgery and cardiac surgery has been expanding, and there is also a great social need for further adaptation of VATS is also increasing be caused it can reduce the burden on patients. However, the problem of post-operative adhesions with VATS has also been reported (15, 49, 50). In VATS where surgical procedure is limited, it is expected that the existence of adhesions will be more problematic than thoracotomy in securing a surgical field. Along with further expansion of operation using VATS, an increase in the demand for re-operative surgery using VATS is well anticipated. But there is a concern that the existence of post-operative adhesions will inhibit various types of procedures such as hemostasis, blunt dissection, and therefore, its prevention is considered to be an important challenge to overcome the problems for the development of VATS. If an insoluble hyaluronic acid can prevent post-thoracotomy adhesion in VATS, it can greatly contribute to the development of VATS. However, insoluble hyaluronic acid is not resistant to damage by rigid instruments such as tweezers or clamps by forceps, and hence, its operability is of a concern in surgeries that require special steel appliances, and involve small incision

wound such as with VATS. Therefore, in Chapter 3 the post-operative adhesion prevention effect and operability of insoluble hyaluronic acid membrane were examined in a limited field of VATS, and not on regular thoracotomy.

In Chapter 4 the detection method of the adhesion prevention effect after thoracotomy was examined. Thoracotomy in dogs is used in various diseases such as mitral valve replacement for treating mitral regurgitation (51), pericardial effusion (52), lung tumor (53) and lobular torsion (54). Dogs are expected to receive advanced medical treatment as companion animals of human, and the number of opportunities for dogs with pleurodesis requiring thoracotomy is expected to increase in the future. The presence or absence of pleurodesis and the site of adhesion in dogs prior to thoracotomy are important in to those who are considering the treatment options. To find out the preventive effect of insoluble hyaluronic acid on post-thoracotomy adhesion examined in Chapter 2 and 3, an examination method which is minimally invasive, with high safety and simple operability is essential. CT exams are known to be effective detection methods of human pleural adhesions (55). Unlike human, it is difficult to adjust the breathing of dogs, thus general anesthesia is required for a CT scan. However, dogs that need re-thoracotomy often exhibit unstable respiration, and it is risky to perform general anesthesia only for examinations. In addition, it is difficult to obtain the dog owner's

informed consent. Therefore, the present study focused on ultrasonic examination (56), which is known as an alternative examination method of pleural adhesions in humans. Ultrasonography is minimally invasive and is trusted as a method for detecting pleural adhesions in human (56). However, since the shape of the thorax is different between dogs and human, it is impossible to use the human ultrasonic pleurodesis detection method in dogs. Therefore, the present study examined whether the human ultrasonography can be applicable to that of dogs, as well as any modifications that should be made on the test method. Hence, the lung sliding of a dog was observed using ultrasonography in mode B, and methods of detecting adhesion between the parietal pleura and pulmonary pleura that align with the shape of a dog's thorax were examined.

Chapter 2

Elucidation of the time-dependent degradation process in insoluble hyaluronic acid formulations with a controlled degradation rate

Introduction

Hyaluronic acid is a biopolymer discovered from the vitreous body of cows in 1934 (28). This molecule is distributed widely throughout the body as part of the extracellular matrix in the cartilage, skin, joints, and elsewhere (29), and has a long history of use as a pharmaceutical product (31-33, 36), with high water retention capacity and safety. Furthermore, because it is degraded in the body, the risk of remaining as a foreign substance in the body for long periods is extremely low. Many issues relating to the mechanisms and rate of degradation are unknown, even though hyaluronic acid is very common material. Thus, studies on hyaluronic acid formulations are ongoing globally.

Adjustment of properties and the degradation rate of hyaluronic acid are also performed by changing the molecular weight (38) and by using crosslinkers (39, 40). Nonetheless, none of the resulting materials are perfect for use *in vivo*, necessitating further development. Although the factors that determine the degradation rate of a hyaluronic acid formulation remain unknown, Park et al. recently reported that a

decrease in swelling ratio may slow the degradation rate of hyaluronic acid formulations (43). However, the factors that determine this swelling ratio are also unclear.

The utility of elucidating the key factors controlling the degradation rate of hyaluronic acid would be incalculable. Moreover, with regard to the hyaluronic acid formulations created using this unknown factor, how many byproducts would arise through the generation process and how the hyaluronic acid formulation would degrade are also crucial elements for new hyaluronic acid formulations.

In this study, the author discovered an approach to controll the swelling ratio with a newly developed method by applying insolubilize sodium hyaluronate without the use of crosslinkers (57). The greatest advantage of this method is that the generated hyaluronic acid formulation does not contain potentially harmful substances such as crosslinkers or modifiers.

Using the above method, the author and my colleagues also created hyaluronic acid formulations with three different swelling ratios and scored the time-dependent morphological changes in hyaluronic acid formulations for each swelling ratio. This *in vivo* degradation was modeled in simulated body fluid (SBF). The results showed that the degradation rate of hyaluronic acid formulation can be controlled by adjusting the swelling ratio.

Materials and methods

Creation of insoluble hyaluronic acid membrane (test membrane)

In accordance with the method described in previous reference (57), a sodium hyaluronate membrane was treated to create an insoluble test membrane. First, correlations between reaction time, swelling ratio, and infrared spectroscopy (IR) spectra were examined. Based on the results of swelling ratio, three groups were created (Group H, high; Group M, moderate; and Group L, low). Three test membranes were prepared for each group.

Measurement of swelling ratio

A 250-mg section of test membrane was cut out and completely immersed in the pure water. The weight of the membrane was measured before and after immersion, and the swelling ratio was determined using the following equation:

swelling ratio = wet weight / dry weight

Infrared spectroscopy analysis

Infrared spectroscopy analysis was conducted using FT-IR equipment (PerkinElmer Japan Co., Ltd., Kanagawa, Japan) with the sample placed in the ATR attachment (Universal ATR sampling Accessory; PerkinElmer). Spectra were scanned four times,

every 2 cm^{-1} from 4000 to 400 cm^{-1}. Peaks were assigned in accordance with a previous report (58).

Creation of SBF

SBF was created following a method described previously (59). In addition, 100 units of penicillin G sodium (Thermo Fisher Scientific, Tokyo, Japan) and 100 μg of streptomycin sulfate (Thermo Fisher Scientific) were added so that the final concentration could be reached. Phenol red was added as a pH indicator to a concentration of 10 mg/L.

Observation of test membrane degradation in SBF over time

A 50-mg section of test membrane was cut out and soaked in a petri dish containing 5 mL of SBF. The test membrane was macroscopically observed once daily and the state of degradation was scored and classified into eight levels (Table 2-1). The diameter of the largest bubble and extent of decay (tubularization) were set as criteria. The number of bubbles was not taken into consideration.

SBF was replaced once every 2-3 days. The pH of SBF was maintained at 7.4 and adjusted using 5 mol/L sodium hydroxide solution (for volumetric analysis standardized

by the Japanese Pharmacopoeia, Wako Pure Chemical 196-05375: FUJIFILM Wako

Table 2-1. Observation of test membrane degradation in SBF over time

Score	Criteria
7	Remain unchanged
6	Bubble diameter less than 1 mm
5	Bubble diameter 1 mm-2 mm
4	Bubble diameter 2 mm-3 mm
3	Bubble diameter over 3 mm
2	Partly tubular
1	Whole tubular
0	Non solid

Criteria for Scoring

Pure Chemical Corporation, Osaka, Japan). Soaking of the test membrane in SBF was started on Day 0, and the test membrane was examined until the score became 0.

Results

Evaluation of insolubilization treatment with IR spectroscopy and swelling rate

Based on a previous report (58), bands at 1600 cm^{-1} and 1390 cm^{-1} belong to C=O and C-O- stretching vibrations of the carboxylate ion (-COO-) of hyaluronan, respectively, and the bands at 1740 cm^{-1} and 1250 cm^{-1} belong to C=O and C-O-H stretching vibrations of carboxylic acid (-COOH), respectively.

Sodium hyaluronate was treated so that different conditions could be examined with treatment times set every 10 minutes from 0 to 90 minutes. Then, the IR and swelling rate were investigated. Two absorption peaks (1600 cm^{-1} and 1410 $cm^{-1} \approx$ 1390 cm^{-1}) belonging to the carboxylate ion are observed in sodium hyaluronate membrane treated for 0 min, but markedly decreased after insolubilization treatment. Furthermore, two new absorption peaks (1740 cm^{-1} and 1250 cm^{-1}) belonging to carboxylic acid appeared with insolubilized membrane (Figure 2-1A). The absorption peak reached a plateau after being treated for 70 min. Based on these results, the 1740 cm^{-1} absorption peak that markedly increased was designated as the index for insolubilization treatment.

Investigation of methods to adjust swelling ratio

Sodium hyaluronate membranes was treated for 30, 60, 90, 120, 150, or 180 min to

create insoluble test membranes, then IR spectra and swelling ratios of these test membranes were examined. Data from the insoluble test membranes were plotted on a graph with transmittance spectra at 1740 cm^{-1} on the horizontal axis (Figure 2-1A) and treatment times on the horizontal axis (Figure 2-1B). Then, these membranes were measured for their swelling ratios with the swelling ratios placed on the vertical axis and the treatment times placed on the vertical axis. There was a strong correlation between swelling ratio and treatment time (Figure 2-1C). Swelling ratios could not be measured because the membranes treated for 0 min were completely absorbed in water and membranes treated for 10 min swelled until they became a gel-like substance.

To investigate the relationship between IR spectra and swelling ratio, a graph was plotted with IR absorption at 1740 cm^{-1} on the vertical axis and swelling ratio on the horizontal axis. A strong correlation was observed between the two variables (R=-0.9826) (Figure 2-1D). These results suggested two things: control of the swelling ratio could be performed by changing the treatment time, and the 1740 cm^{-1} absorption peak of IR is a predictable indicator of the swelling rate.

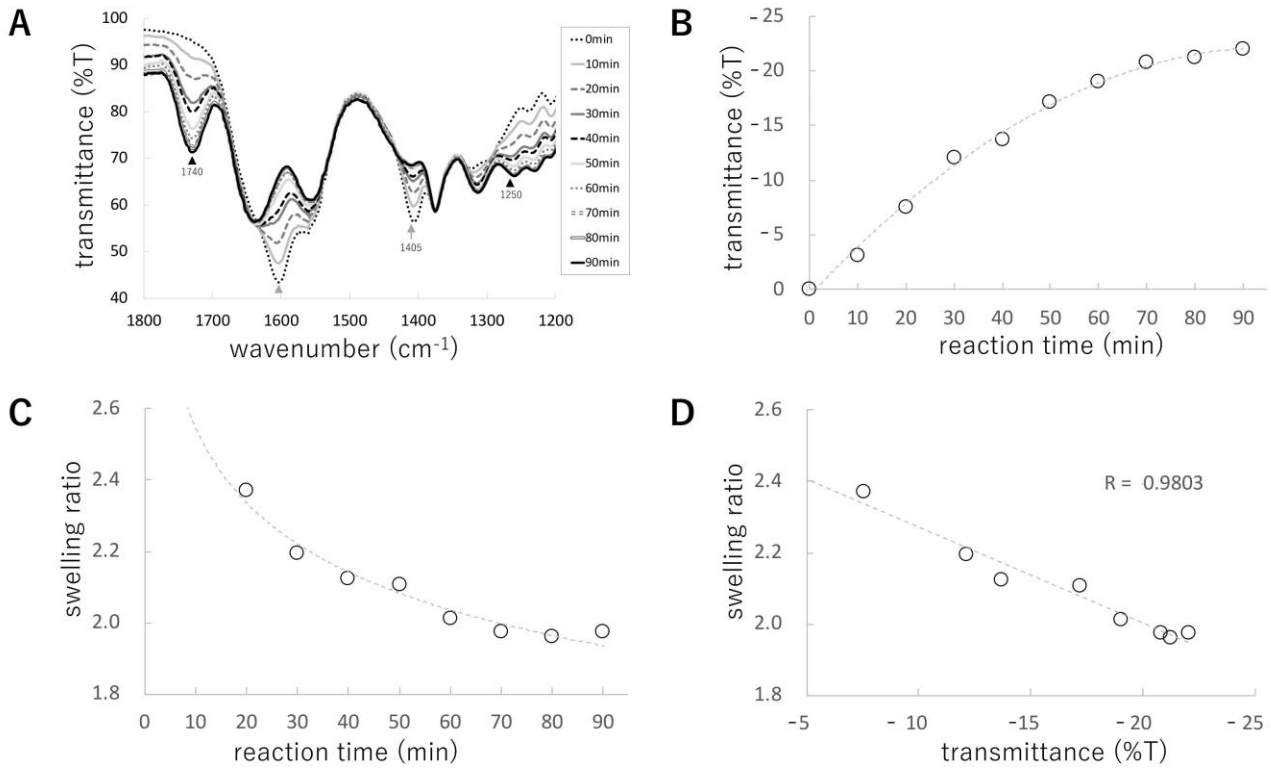

Figure 2-1. Effect of insolubilization treatment on IR spectra of hyaluronic acid

(A) Changes in IR spectra by insolubilization treatment time (0-90 min). Absorption peaks belonging to carboxylate ion (1600 and 1410 cm^{-1}) decreased and the two absorption peaks belonging to carboxylic acid (1740 and 1250 cm^{-1}) increased proportionally with treatment time. The absorption peak reached a plateau after treatment of 70 min.

(B) Graph of the treatment time and IR spectra. Transmittance spectra of 1740 cm^{-1} were plotted on the vertical axis and treatment time on the horizontal axis.

(C) Graph of the treatment time versus IR spectra. Changes in swelling ratio by insolubilization treatment time (0-180 min). Swelling ratio decreased inversely proportional to treatment time. With approximately 90 min of treatment, the decrease in swelling ratio reached a plateau.

(D) Graph of IR absorption at 1740 cm^{-1} and swelling ratio. A strong correlation was observed between the two variables (R=0.9803).

Creation of test membranes for investigating degradation process

Based on the results obtained (Figure 2-1), three types of insoluble hyaluronic acid membrane with different swelling ratios (three for each type) were created: Group H, high swelling ratio (2.58, 2.42, 2.42); Group M, moderate swelling ratio (2.02, 2.23, 2.22); and Group L, low swelling ratio (2.00, 1.97, 2.05). These membranes were used in the investigations of degradation process described below.

Observation of test membrane degradation in SBF over time

Up until Day 1, none of the test membrane groups exhibited changes and all had a score of 7. On Day 2, the score for Group H with the greatest swelling ratio began to decline. No changes in Groups M or L were observed at this point. Score began to decrease on Day 3 or 4 for Group M and Days 5-11 for Group L. Score reached 0 on Day 14 or 15 in Group H, Day 15 for all three membranes in Group M, and Day 16 for all three membranes in Group L. All groups showed a similar trend in changes until complete disappearance after the score was ≤6, when morphological changes of the membrane appeared (Figure 2-2A). In addition, there is a strong correlation between score and swelling ratio (Figure 2-2B).

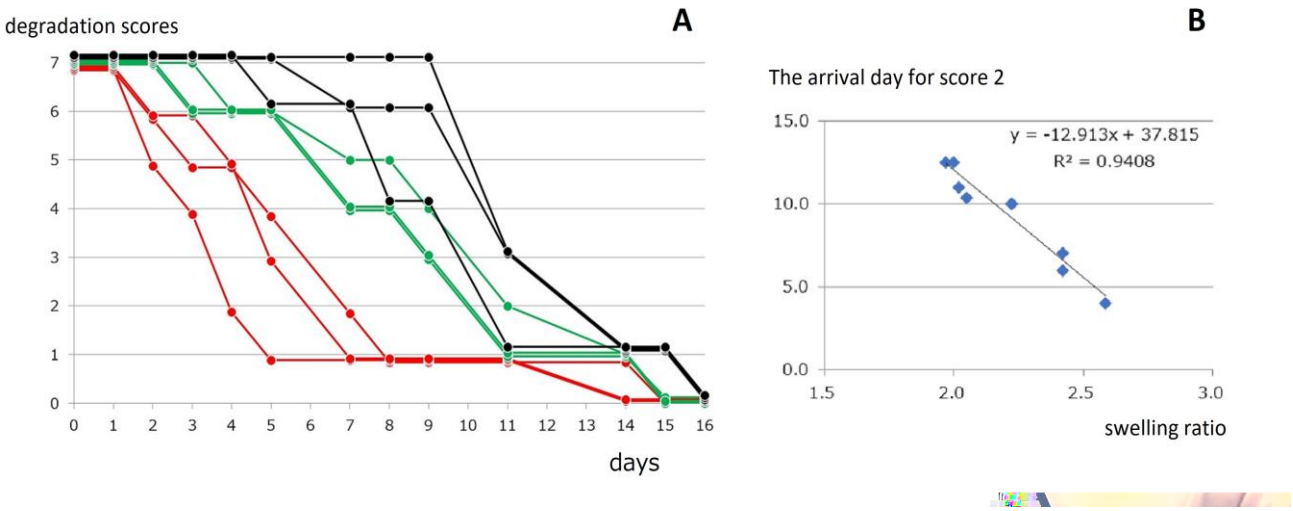

Figure 2-2. Swelling ratios and degradation scores

(A) Low swelling ratio led to early decomposition. All groups showed a similar trend in changes until complete disappearance after the score reached ≤ 6, and morphological changes appeared in the membrane. (Score 7, Remain unchanged; Score 6, Bubble diameter less than 1 mm; Score 5, Bubble diameter 1 mm-2 mm; Score 4, Bubble diameter 2 mm-3 mm; Score 3, Bubble diameter over 3 mm; Score 2, Partly tubular; Score 1, Whole tubular; Score 0, Non solid)

(B) The arrival day for score 2 and swelling ratio. Score and swelling ratio have a strong correlation (R2=0.9408).

The present study observed the following changes in the test membrane that were proportionate to the treatment time for insolubilized sodium hyaluronate:

1) Decreased swelling ratio

2) Decreased absorption at 1600 cm^{-1} and 1405 cm^{-1} belonging to carboxylate ions, and increased absorption at 1740 cm^{-1} and 1250 cm^{-1} belonging to carboxylic acid on the IR spectra

3) Delayed degradation in SBF

These results demonstrated that swelling ratio, IR absorption peaks assigned to carboxylic acid/carboxylate ion, and degradation rate are correlated with each other.

Park et al. reported the feasibility of slowing the degradation rate of hyaluronic acid formulations by decreasing the swelling ratio (43). However, what affected the swelling ratio itself was unknown. The present results suggest that hydrogen bonds are an important factor in the swelling ratio that determines the degradation rate. The author also verified with NMR that new covalent bonds and side chains had not formed before and after the insolubilization treatment (data not shown). This strongly suggested that byproducts such as modifiers and crosslinkers had not emerged. That is, the degradation rate of the test membrane can be controlled, and a highly safe formulation that does not contain substances other than hyaluronic acid and sodium hyaluronate can be generated.

The author has previously reported that test membrane exhibited a clear effect in preventing postthoracotomy pleural adhesions in dogs (64, 65). The finding from this study that the swelling ratio and degradation rate of hyaluronic acid formulation can be controlled is an extremely beneficial feature for hyaluronic acid formulations. Furthermore, improvements in many products, not only preventive materials for postoperative adhesions, but also pharmaceutical products such as osteoarthritis treatments and cosmetic medicines, can be anticipated to take advantage of these properties.

The limitations of this study were as follows. The test substance is in the form of a membrane, which may be unsuitable for use as an injectable material under the present circumstances. However, the form of the substance may well be amenable to change when drying during the generation process. That is the formulation may be able to be modified into specific shapes, such as a small particles, string, or tubes rather than membranes during the process of drying the hyaluronic acid formulation. Since this would affect the clinical application such as the target disease and purpose of use, further investigations will be conducted in the future.

Conclusions

In conclusion, the present study identified the swelling ratio of hyaluronic acid formulations as a controllable factor. It suggested the correlations between IR absorption peak at 1740 cm^{-1} and swelling ratio, and between IR absorption peak at 1740 cm^{-1} and degradation speed. In addition, hyaluronic acid formulations appear to degrade gradually with time. Generated hyaluronic acid formulations showed no byproducts through the generation process. Further studies are needed in order to identify further changing forms and reactions that could be achieved *in vivo*. However, the present study demonstrated a novel approach to hyaluronic acid formulations which can be applicable to clinical use.

Chapter 3

Development of an Anti-Adhesive Membrane for Use in Video-Assisted Thoracic Surgery

Introduction

In chapter 2, the factors controlling the degradation rate of hyaluronic acid, as well as the degradation process, was elucidated the shape will be maintained without degradation in simulated body fluid for about seven days, and the period of time during which adhesions form postoperatively. In this chapter, the application of the insoluble hyaluronic acid membrane for video-assisted thoracic surgery (VATS) was evaluated.

VATS which has become more common in recent years as a minimally invasive treatment approach, is now adapted in a variety of procedures including respiratory surgery and cardiac surgery, and its problems with postoperative adhesions are also described in VATS (15, 49). The surgical manoeuvers available in VATS are restricted, and the presence of adhesions is predicted to be a severe problem, because the surgical field of view is limited compared with thoracotomy. By further application of VATS to various kinds of operative procedures, an increase in demand for repeated operations under VATS procedure may be expected. Although VATS is less invasive and causes

less postoperative adhesions than standard thoracotomy, still any small adhesion may interrupt the operation. From the standpoint of VATS development in the future, the prevention of postoperative adhesions should be the major challenge. It is predicted that materials highly effective in preventing postoperative adhesions after thoracic surgery can be used in VATS with a small incision of about 3-6 cm (66), which will become essential in cardiac and respiratory surgeries. In the author's previous study, when a large incision was made in situations such as thoracotomy, it was able to cover the whole target site by inserting the membrane into the thoracic cavity after gently folding the test membrane in half. It can be spread with gauze balls. However, because the membrane was not strong enough to withstand damage caused by solid instruments such as tweezers and forceps, their mactical use in VATS surgery needs to be evaluated. Thus, in Chapter 3, this study examines the operability, safety, and efficacy of an anti-adhesive insoluble hyaluronic acid membrane in VATS.

Materials and Methods

This study was approved by the Institutional Animal Care and Use Committee of Tokyo University of Agriculture and Technology (Permit number 27-36). All treatments involving experimental animals were conducted in accordance with the Animal Experiments Subcommittee of Tokyo University of Agriculture and Technology and the Guide for the Care and Use of Laboratory Animals Eighth Edition (Committee for the Update of the Guide for the Care and Use of Laboratory Animals; National Research Council).

Test membrane implantation

Ten male TOYO beagles (9.8-10.5 kg) were purchased from Kitayama Labs Co. Ltd. (Nagano, Japan). The experiment consisted of two groups: the experimental group and the control group (n=5 each). Animals were given cefovecin sodium (8 mg/kg, sc; Convenia®, Zoetis Japan Inc., Tokyo, Japan) to prevent infection and buprenorphine (0.02 mg/kg, sc; Buprenorphine for injection 0.2 mg, Nissin Pharmaceutical Co., Ltd., Tokyo, Japan) for analgesia. Subsequently, animals were pre-treated with atropine sulphate, butorphanol tartrate (0.2 mg/kg, iv; Vetorphale®, Meiji Seika Pharma Co., Ltd., Tokyo, Japan), and midazolam (0.2 mg/kg, iv; Midazolam injection [SANDOZ], Sandoz K.K., Tokyo, Japan), followed by general anaesthesia induction with propofol (6

mg/kg, iv; “Mylan,” Mylan Inc., Tokyo, Japan). Following tracheal intubation, anaesthesia was maintained with isoflurane inhalation (1-2%, Isoflurane for animals, Intervet K.K., Tokyo, Japan). Respiratory management was performed with manual bag-mask ventilation and intermittent positive pressure breathing through an artificial anaesthesia device.

An insoluble hyaluronic acid membrane containing glycerol was used as the test membrane (100 mm x 100 mm x 1.0 mm). The test membrane was implanted in the left thoracic cavity of the animal under VATS. A 12-mm-diameter port was created at the tenth intercostal space on the left side with a trocar, and a 35-mm-diameter small incision for operation was subsequently created at the fifth intercostal space on the left side under video camera monitoring. A wound protector (for 35-mm-diameter incisions) (Wrap Protector FF0707, Hakko Co., Ltd., Nagano, Japan) was inserted at the small incision for operation. Intercostal nerve block was performed in advance with bupivacaine (Marcaine injection 0.5%, AstraZeneca plc, Osaka, Japan) for port and small incision sites. An automatic suture device (Endo GIA, 45 mm, Covidien Japan Inc., Tokyo, Japan) was inserted from the port at the tenth intercostal space. Grasping forceps were then inserted from the small incision to hold the lung parenchyma, and the automatic suture device was used for stapling and dissection. Then, dissected lung tissue

was removed from the small incision. In the experimental group, after the adhesion-preventing membrane was inserted from the small incision and placed between the visceral pleura and parietal pleura, a drain tube (Phycon tube SH No.3: 2.5 mm inner diameter, 4.0 mm outer diameter, Fuji Systems Corporation, Tokyo, Japan) was inserted. After gradually re-expanding the lung lobes, the trocar was removed. The wound was closed using 2/0 synthetic absorbable suture (Biosyn, Covidien Japan Inc.) using a conventional method. For the control group, a similar procedure was used without inserting the adhesion-preventing membrane, and the wound was subsequently closed.

Any abnormalities such as pneumothorax and pleural effusion were checked on the day after surgery. Pleural effusions were removed, if present, once a day, and their volumes were recorded. Chest drains were removed when pleural effusions were no longer observed.

At postoperative week 2, animals were anaesthetized similarly to the operation for membrane insertion and then euthanized with an overdose of potassium chloride solution under deep general anaesthesia. Subsequently, blood was removed, and the chest was re-opened with median sternotomy.

4.2. Observation and test methods

In all animals, general condition, appetite, and vigour were checked and recorded once a day (animals were observed before implantation and after awakening from anaesthesia on the day of implantation). The day of implantation was specified as day 1 of observation.

At the time of sacrifice when the chest was re-opened, adhesions, if present, were dissected macroscopically using Kelly forceps, Metzenbaum scissors, and cotton swabs, and the strength of adhesion was evaluated and scored based on the degree of bluntness or sharpness of the dissection process (0=no need to dissect; 1=film-like adhesion, can be dissected easily; 2=mild adhesion, can be dissected; 3=moderate adhesion, difficult to dissect; 4=strong adhesion, impossible to dissect).

For histological examination, parietal pleura and lung samples were collected near the test membrane insertion site. Removed pleural and lung tissues were fixed in 10% neutral buffered formalin solution for one week at room temperature. After fixation, intercostal tissues were cut perpendicularly from the parietal to the visceral direction to create slice tissue samples that were embedded in paraffin blocks. After sectioning, samples were stained with hematoxylin and eosin (HE). Under an optical microscope, histopathological lesions were categorized according to the criteria for histopathological

classification described below, and images of a representative view for each finding were taken. To compare the effects of the test membrane in preventing adhesions, the adhesion site and dorsal aspect of the lungs (including visceral pleura) were histopathologically evaluated in terms of tissue adhesion, fibrosis, mesothelial cell hypertrophy, cuboidal epithelialization of type II alveolar epithelial cells, and mononuclear cell infiltration, in animals with adhesions between the lung and chest wall and in animals with interlobular adhesions. In animals without adhesions, the dorsal aspect of the lungs (including visceral pleura) was similarly evaluated.

The criteria for histopathological classification were the following: (adhesion: –, absent; +, present), (fibrosis in pleura: +, localised; ++, diffuse), (mesothelial cell hypertrophy in pleura: –, absent; +, mild), (alveolar epithelial cell cuboidal epithelialization in alveoli: –, absent; +, localised; ++, diffuse), (mononuclear cell infiltration in alveoli: –, absent; +, localised), and (mononuclear cell infiltration in interstitium: –, absent; +, localised; ++, diffuse).

Results

Insertion of an adhesion prevention membrane

After immersion in saline, the membrane became rapidly and sufficiently pliable, and it was not cracked by normal handling. In one animal (E4), the membrane was torn into multiple pieces while delivering it from the small ~3.5-cm incision for left-sided VATS to the thoracic cavity, making it difficult to completely cover the target site. Membrane insertion in all other animals in the experimental group was achieved successfully (Figure 3-1). Moreover, there were no differences in operability with wet gloves or with a wet wound protector placed at the small incision site. The membrane did not hinder the chest closing procedure.

Postoperative general condition

All animals showed satisfactory awakening from anaesthesia. No abnormalities in general condition, such as vigour, appetite, and respiratory condition, were observed during follow-up. Chest drains were removed when pleural effusions were no longer observed (observation days 2-3).

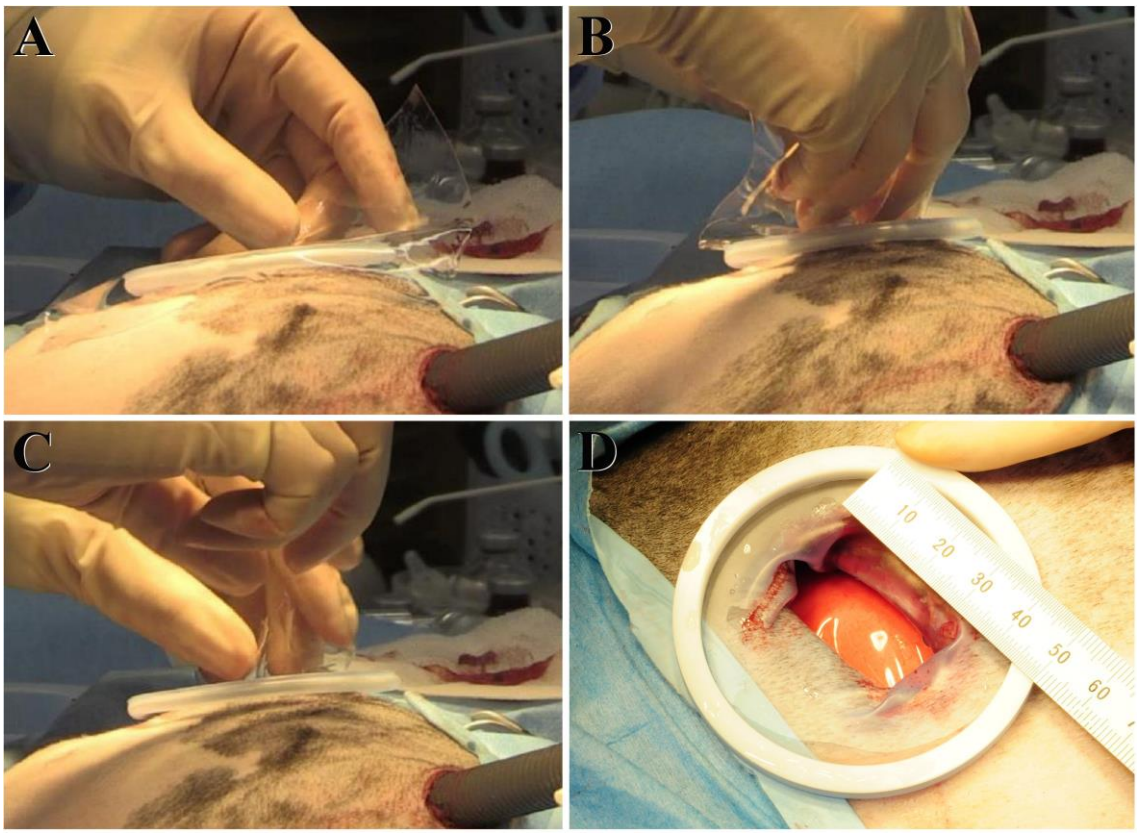

Figure 3-1. Membrane insertion procedure

In the experimental group, the adhesion-preventing membrane is inserted from the small incision and placed between the visceral pleura and parietal pleura. Membrane insertion in all animals except for E4 in the experimental group was achieved successfully in the order of panel A to panel D.

Macroscopic findings after thoracotomy

In the experimental group, adhesions were observed between the chest wall and lungs in 2/5 animals, and blunt dissection of the adhesions was difficult to achieve in one animal (E4) (adhesion scores: 3 for E4, 0 for E5, 2 for E6, 0 for E7, and 0 for C10). Pulmonary interlobular adhesions were observed in 2/5 animals, but blunt dissection could be achieved in all adhesions (adhesion scores: 0 for E4, 0 for E5, 0 for E6, 2 for E7, and 2 for E10). The median adhesion score was 0. In the control group, adhesions were observed between the chest wall and lungs in 3/5 animals, and blunt dissection of the adhesions was difficult to achieve in one animal (C2) (adhesion scores: 0 for C1, 3 for C2, 0 for C3, 1 for C8, and 1 for C9). Interlobular adhesions were observed in all 5/5 animals, and blunt dissection was difficult to achieve in 4 animals (adhesion scores: 3 for C1, 3 for C2, 2 for C3, 4 for C8, and 3 for C9). The median adhesion score was 2.5 (Table 3-1). In both the implant group and the control group, adhesions were completely absent at the VATS insertion port (tenth dorsal intercostal space).

With regard to pleural effusions, 4/5 animals in the experimental group (excluding E4) showed pale yellow, viscous pleural effusions (90-110 mL/dog) (Figure 3-2). Pleural effusions were not observed in the control group.

Table 3-1. Macroscopic findings of adhesion after thoracotomy

	Control group	Experimental group
No. of animals examined	5	5
Adhesion score		
Between the chest wall and lungs (1/2/3/4)	3 (2/0/1/0)	2 (0/1/1/0)
Pulmonary interlobular adhesions (1/2/3/4)	5 (0/1/3/1)	2 (0/2/0/0)
Median adhesion score	2.5	0.0

Adhesion scores: the degree of bluntness or sharpness of the dissection process (0, no need to dissect; 1, film-like adhesion, can be dissected easily; 2, mild adhesion, can be dissected; 3, moderate adhesion, difficult to dissect; 4: strong adhesion, impossible to dissect).

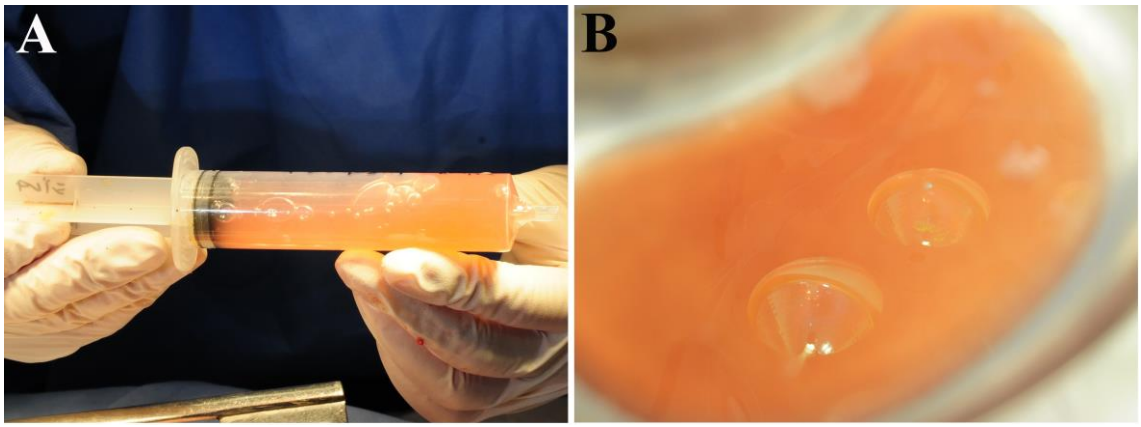

Figure 3-2. Pleural effusions observed at the re-thoracotomy

Four out of five animals in the experimental group (excluding E4) showed pale yellow, viscous pleural effusions (90-110 mL/dog).

Histopathological evaluation

There were no obvious difference between the experimental group and the control group in the incidence or severity of adhesion of lung and chest wall, pulmonary interlobular adhesion, pleura fibrosis (Figure. 3-3A and B), pleura mesothelial cell hypertrophy (Figure. 3-3C and D), alveolar epithelial cell cuboidal epithelialization (Figure. 3-3E and F), alveolar mononuclear cell infiltration (Figure. 3-3E and F), and interstitial mononuclear cell infiltration (Table 3-2).

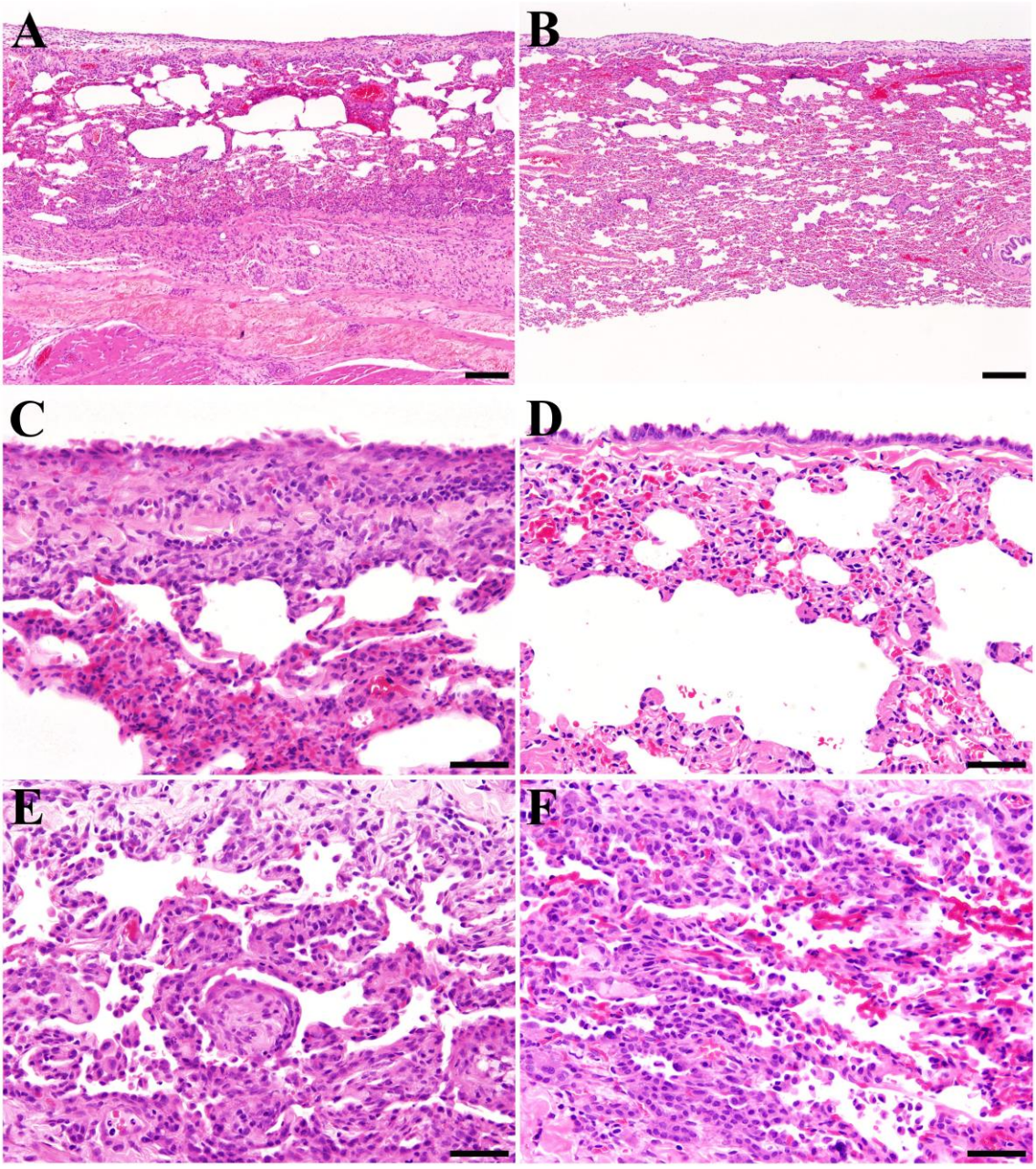

Figure 3-3. Histopathological changes in the chest wall and lungs at the re-thoracotomy

The test membrane elicits only a minor inflammatory response and foreign body reaction compared with the control group. (A, B) Pleural fibrosis (++) in a control animal (A) and an experimental group animal (B). (C, D) Mesothelial cell hypertrophy (+) in a control animal (C) and an experimental group animal (D). (E, F) Alveolar epithelial cell cuboidal epithelialization (+) and mononuclear cell infiltration (+) in a control animal (E) and an experimental group animal (F).

(A–F: Hematoxylin and eosin staining. Bar: A, B = 200 μm, C–F = 50 μm.

Table 3-2. Incidence of histopathological changes appeared in the left lung and left chest wall

	Control group	Experimental group
No. of animals examined	5	5
Adhesions		
Lung and chest wall (+)	1 (1)	2 (2)
Pulmonary interlobular (+)	3 (3)	2 (2)
Pleura		
Fibrosis (+/++)	5 (2/3)	5 (0/5)
Mesothelial cell hypertrophy (+)	4 (4)	5 (5)
Alveoli		
Epithelial cell cuboidal epithelialization (+/++)	3 (3/0)	5 (4/1)
Mononuclear cell infiltration (+)	3 (3)	1 (1)
Interstitium		
Mononuclear cell infiltration (+/++)	4 (4/0)	3 (2/1)

Criteria for histopathological classification: Adhesions: +, present; Fibrosis in the pleura: +, localised; ++, diffuse; Mesothelial cell hypertrophy in the pleura: +, mild; Alveolar epithelial cell cuboidal epithelialization: +, localised; ++, diffuse; Alveolar mononuclear cell infiltration: +, localised; Interstitial mononuclear cell infiltration: +, localised; ++, diffuse.

Discussion

One of the major differences between thoracotomy and VATS is the size of the incisions associated with the surgery. VATS is a minimally-invasive procedure that involves small incisions; for instance, the incision size to remove resected lung lobes is limited to 3-6 cm (66). In surgical treatment using anti-adhesive membranes under VATS, the insoluble hyaluronic acid membrane becomes flexible for easy handling with a high moisture content by immersing it in saline immediately before use. However, it can be cracked and torn into multiple pieces if it is completely folded; thus, it is not practical to fold the membrane prior to insertion through the small incision. In fact, in one animal of the experimental group (E4), the membrane tore into several pieces during its delivery from the small incision to the thoracic cavity, and complete coverage of the target site could not be achieved. However, it was possible to insert the test membrane by grasping the four corners of the test membrane. With this procedure, the membrane forms a drawstring pouch and can be dropped into the thoracic cavity by pushing the centre of the membrane into the thoracic cavity, without folding it from the small incision. Similar to the procedure for thoracotomy, the membrane could cover the target site successfully in the thoracic cavity using standard surgical instruments. Although it is necessary to have some experience to insert the membrane from a small

incision, the technique does not require strict skill. The membrane can also be placed successfully by inserting and simply “dropping” it into the thoracic cavity. Moreover, this procedure can be achieved with both wet and dry surgical instruments and gloves. The membrane showed adhesion-preventing effects simply by placing the membrane without attachment to wrap the target site. From this point of view, this membrane was superior to the carboxymethyl-cellulose membrane for laparoscopy use. The size of the small incision created in the present study (~3.5 cm) was similar to the typical size of incision that is created to remove pulmonary lobes in clinical lobectomy (66), indicating that this membrane can be used in a practical manner in VATS in the clinical setting.

In the experimental group, only one animal (E4) developed an adhesion (left chest wall and lung) with an adhesion score of 3 (blunt dissection of the adhesion difficult to achieve), which can be clinically problematic with VATS. In this animal, the test membrane cracked during insertion, and was torn into multiple pieces. The reason for the development of the clinically problematic adhesion was insufficient coverage of the target site. This animal did not show a pleural effusion at sacrifice. This was because the test membrane was manufactured by applying surface water induction technology, which enables integration of water by glycerol and then absorption of a large amount of water by insoluble hyaluronic acid to create a barrier (25). Consequently, this physical

property of this test membrane enables prevention of adhesions between the chest wall and lung. As possible causes of the development of adhesions, the test membrane may lose its physical properties as a barrier. By cracking the membrane during insertion, this membrane loses its surface water induction property, and the uncovered portion may develop adhesion. In fact, adhesions were completely absent at the left-sided VATS insertion port (tenth dorsal intercostal space) in both the implant and control groups. The lack of apparent adhesion at the insertion port may be due to extremely active lung movement by respiration and the extremely small incision.

In the macroscopic examination at sacrifice, no exudative changes suggestive of inflammatory responses were observed in the thoracic cavity in the experimental group. Histopathological analysis also showed no apparent induction of inflammatory changes or a foreign body reaction. This result suggests that the test membrane dissolves spontaneously within the thoracic cavity to be absorbed into the body and does not remain as a foreign substance, thus not causing an inflammatory response or foreign body reaction. Although the chest drain was removed a few days postoperatively when a pleural effusion was no longer observed, a pale yellow pleural effusion (90-110 mL/dog) was observed in 4/5 animals in the experimental group at sacrifice. This pale yellow pleural effusion might be generated during the process to dissolve and absorb the

test membrane. In human medicine, the clinical symptoms of pleural effusions are considered to be dependent on the underlying lung disease (67-69), and the pleural effusion observed in the present study would be unlikely to become a problem in the clinical setting.

The extent of surgical invasiveness is one of the important issues that must be addressed. While postoperative adhesions after thoracic surgery occurs at a high rate (5-7, 9), the incidence of adhesions depends on the intraoperative invasiveness of the surgical procedure. In the present study, only wedge resection of the lung lobe was performed using an automatic suture device. In this procedure, intraoperative tissue dissection was not necessary, and only a small amount of bleeding can be expected with this procedure. This is the reason for the fewer adhesions that occurred even in the control group and VATS is less invasive than thoracotomy. As future investigations, induction of adhesions will need to be compared between use and non-use of the test membrane in surgeries with a greater degree of invasiveness, such as lobectomy or pericardial incision, instead of wedge resection.

Conclusions

In conclusion, the test membrane used in this study showed satisfactory operability not only in typical thoracotomy, but also in VATS, which is becoming increasingly common. Its easy delivery and spread within the thoracic cavity may be well suited for VATS procedures. This test membrane elicited only a minor inflammatory response and foreign body reaction and appears to be practical as a material to prevent postoperative adhesions after thoracic surgery and VATS.

Chapter 4

Utility of lung ultrasound for detection of pleural adhesions in dogs

Introduction

In chapter 2, it was elucidated the time-dependent degradation process in insoluble hyaluronic acid formulations with a controlled degradation rate. In chapter 3, it was indicated that the novel anti-adhesive membrane was effective and safety in preventing pleural adhesions. In this chapter, the new method for detecting pleural adhesion after thoracic surgery was evaluated.

There is a high incidence of pleural adhesions after thoracic surgery or in thoracic diseases such as lung cancer (70) and lung abscess (71). Although it is uncommon for pleural adhesions to cause organ disorders in humans (72), increased risk during thoracotomy is one of the significant problems in patients with pleural adhesions. Specifically, it has been known in humans for many years that prolonged duration of surgery, increased blood loss, poor field of view, and pulmonary vascular injuries occur due to postoperative adhesions between the thoracic wall and the lung(5-9).

Thoracotomy is also performed in dogs to treat various conditions such as mitral regurgitation (51), pericardial effusion (52), lung tumor (53), and lung lobe torsion (54).

As members of a family, dogs have come to undergo advanced medical treatments, and an increasing number of thoracotomies may be predicted in dogs with pleural adhesions in the future. Preoperative identification of the presence and location of pleural adhesions is essential for a safe approach in canine thoracotomy. A minimally-invasive approach such as video-assisted thoracic surgery (VATS) has also become popular in the veterinary field (73, 74), and the preoperative detection of pleural adhesions is extremely useful, since it is crucial to ensure the surgical field of view in this procedure (75).

Some of the desired features of a procedure for detecting these pleural adhesions include minimal invasiveness, high safety, and simple yet convenient operability. One of the useful methods for detecting pleural adhesions in humans is computed tomography (CT) (55). CT uses a computer to process tomographic images, allowing for three-dimensional visualization of the intrathoracic condition. However, there are several issues with CT examinations. Reports have shown that human patients, as well as some dogs, with a history of interventional vascular embolization (coils) are at higher risk of inaccurate diagnosis as a result of metal artifacts (76). CT has also been reported to cause pacemaker malfunction in humans (77), and this complication may occur in veterinary medicine. CT scanners are unfamiliar to primary veterinary care facilities,

and facilities that can own such equipment are limited. Even for facilities with CT scanners, proper interpretation of the results requires extensive training.

Ultrasound examination is another method that can be used for the assessment of pleural adhesions in humans (56). It has been reported to be safe, effective, cost-effective, and particularly useful in preoperative examinations for VATS in humans (78, 79). In addition, the adhesions can be evaluated with B-mode only, without Doppler function, and ultrasound examinations are available at primary care facilities and small clinics. Furthermore, advanced interpretation skills are not necessary, since it is only used to confirm the presence or absence of lung sliding. However, the ultrasound method to identify human pleural adhesions cannot be applied directly to dogs due to differences in the shape of the thorax between dogs and humans.

In the present study, lung respiratory movement (“lung sliding”) was examined in dogs using B-mode on ultrasound, and a method that assesses adhesions between the parietal pleura and the lung (pulmonary pleura), adjusting for the shape of the canine thorax, was evaluated. The results and the effectiveness of lung ultrasound are presented.

Materials and Methods

This study was approved by the Institutional Animal Care and Use Committee of Tokyo University of Agriculture and Technology (Permit number 27-36). All treatments in experimental animals were conducted in accordance with the Regulations on Animal Experiments of Tokyo University of Agriculture and Technology and the Guide for the Care and Use of Laboratory Animals Eighth Edition (Committee for the Update of the Guide for the Care and Use of Laboratory Animals; National Research Council).

First, lung ultrasound was performed under general anesthesia, followed by thoracotomy. Two weeks after thoracotomy, lung ultrasound was repeated under general anesthesia. Subsequently, the animals were sacrificed, and thoracotomy was again performed to determine the status of pleural adhesions. The detailed procedure is described below.

Animal Preparation

Seventeen male beagles (TOYO Beagles; KITAYAMA LABES, Nagano, Japan) were used in this study.

Anesthesia

The animals were given cefovecin sodium (8 mg/kg, sc; Convenia, Zoetis Japan Inc., Tokyo, Japan) to prevent infection and buprenorphine (0.02 mg/kg, sc; Buprenorphine for injection 0.2 mg, Nissin Pharmaceutical, Tokyo, Japan) for analgesia. Subsequently, the animals were pre-treated with atropine sulfate, butorphanol tartrate (0.2 mg/kg, iv; Vetorphale R, Meiji Seika Pharma Co., Ltd., Tokyo, Japan), and midazolam (0.2 mg/kg, iv; Midazolam injection [SANDOZ], Sandoz, Tokyo, Japan), followed by propofol (6 mg/kg, iv; "Mylan," Mylan Inc., Tokyo, Japan) for induction of general anesthesia. Following tracheal intubation, anesthesia was maintained with isoflurane inhalation (1-2%, Isoflurane for animals, Intervet K.K., Tokyo, Japan). Respiratory management was performed with intermittent positive pressure ventilation through an artificial anesthesia device. During lung ultrasound examination, the inspiratory pressure was set at 20 mmHg to induce exaggerated respiration under forced ventilation with a respiratory rate of 12 breaths per minute and I (inspiration):E (expiration)=1:1, but without positive end-expiratory pressure (PEEP).

Ultrasound Scanning

Lung sliding assessments and adhesion examinations were performed using lung ultrasound. This method has been patented in Japan (PATENT NUMBER 6115958).

After anesthesia induction, lung ultrasound examination was performed in a general operating room. The presence or absence of adhesions was determined noninvasively using an F75 ultrasound system (Hitachi Aloka Medical, Ltd, Tokyo, Japan) and a linear probe (Aloka UST-5412, center frequency of 12 MHz, adjustable frequency range of 10 to 14 MHz). To examine pleural adhesions on the left side, the animal was placed in a right lateral recumbent position and shaved from the first to thirteenth rib on the left thoracic wall. Similarly to a previously reported method (79, 80), B-mode was used, and the probe was pressed perpendicularly to the left thoracic wall such that the reference marker faced the caudal side. The probe was kept in a fixed position when placed on the chest of the dog. To examine adhesions on the right side, the animal was placed in a left lateral recumbent position, and the probe was pressed perpendicularly to the right thoracic wall in a similar manner as above (Figure 4-1).

The sites observed were the third to sixth intercostal spaces of the thoracic wall on both sides at the dorsal line (at the kidney level) and at the ventral line (approximately 5 cm dorsal to the costochondral joint). A total of 16 sites (8 on each side) per animal were examined.

The pleural movements of two consecutive respirations were recorded in the format of still images and videos. The presence or absence of adhesions was determined based

Figure 4-1. Examining adhesions on the left side

The animal is placed in a right lateral recumbent position, and the probe is pressed perpendicular to the left thoracic wall.

on the presence or absence of sites that showed disappearance of respiratory movement (lung sliding) of the parietal pleura and visceral pleura. Lung sliding was checked at every intercostal space. Lung sliding was scored on a four-level scale based on the percentage of the total area that showed lung sliding (3: lung sliding observed in roughly 80% or greater of the total area of the intercostal space; 2: movement observed in about 50% of the total area of the intercostal space; 1: movement observed in a small area of the intercostal space; 0: movement absent) (Figure 4-2). For example, when the 4th intercostal space was checked at the dorsal line, the probe was kept fixed in the 4th intercostal space at the kidney level, and if movement was observed in 80% of the total area from the caudal 4th costal to the cranial 5th costal, the lung sliding score was 3. On inter-session analysis, the kappa statistic of the lung sliding score was 0.656577, while on intra-session analysis (performed by the same assessor on a different day), the kappa statistic was 0.866489. With lung sliding scores of 0, 1, and 2, adhesion was considered present, while a score of 3 was taken as indicating the absence of adhesion.

Thoracotomy

After opening the chest with an incision of approximately 10 cm at the fifth intercostal space on both sides and exposing the area to air for 30 minutes, an insoluble

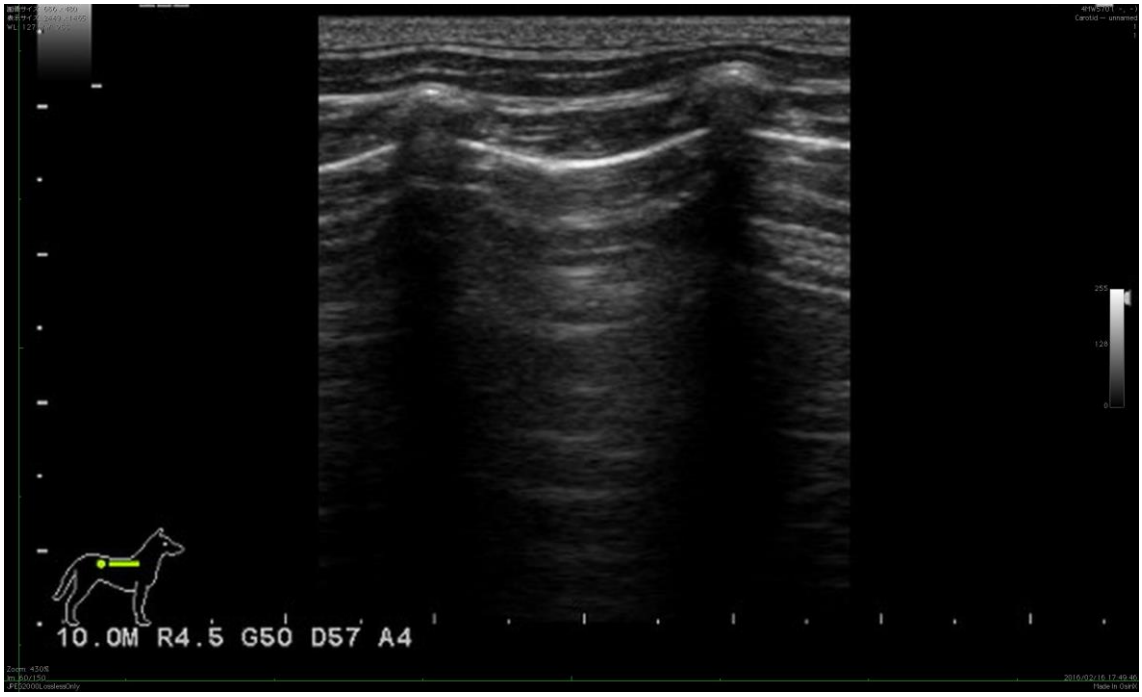

Figure 4-2. Lung Sliding

Lung sliding was scored on a four-level scale based on the percentage of the total area that showed lung sliding.

hyaluronic acid membrane was placed on the visceral pleura of the incision wound to prevent adhesions. The chest was subsequently closed using a standard method.

Necropsy

Two weeks after the initial lung ultrasound and thoracotomy, lung ultrasound was again performed under the same anesthesia conditions as the initial thoracotomy before sacrifice. The animals were subsequently sacrificed with an overdose of potassium chloride (KCL Injection 20 mEq Kit; Terumo Co., Ltd., Tokyo, Japan) under deep general anesthesia. Necropsy was performed with a median sternotomy to determine the presence or absence of adhesions in the thoracic cavity, and sites with adhesions were examined carefully.

Statistical approach

The presence/absence of adhesions was compared statistically by comparing the lung sliding score of the parts with adhesion and the lung sliding score of the parts with no adhesion using the Mann-Whitney U test.

Results

Visualization of the pleural line at any examination site was possible in all dogs. Visualization of lung sliding was performed by simply pressing the probe vertically against the intercostal region, without any additional movement or rotation of the probe (i.e. it is necessary to keep it in a fixed position). The lung ultrasound findings were compared with adhesion findings at necropsy. The median lung sliding score of the 12 sites that showed pleural adhesions was 1.5. The median lung sliding score of the 532 sites that did not show pleural adhesions was 3.0. The lung sliding score was significantly lower in the presence of adhesions ($P<0.0001$, Mann-Whitney test). The sites with pleural adhesions observed with thoracotomy coincided with the sites with decreased lung sliding scores on lung ultrasound (Table 4-1).

The sensitivity and specificity for detecting pleural adhesions with the lung sliding score were determined. Of the 77 sites with an adhesion determined by a lung sliding score of ≤ 2, adhesions were present in 12 sites and absent in 65 sites on macroscopic examination at necropsy. Of the 467 sites without an adhesion, determined by a lung sliding score of 3, adhesions were present in 0 sites and absent in 467 sites on macroscopic examination at necropsy. Based on these results, the ultrasound examination detected pleural adhesions with a sensitivity of 100.0% and a specificity of

Table 4-1. Lung sliding scores on lung ultrasound

		Macroscopic findings of adhesions	
		Present	Not present
	No. of experimental parts	12	532
Lung sliding score			
Intercostal 3	dorsal (0/1/2/3)	(0/0/0/0)	(0/0/6/62)
	ventral (0/1/2/3)	(0/0/0/0)	(0/0/24/44)
Intercostal 4	dorsal (0/1/2/3)	(0/0/0/0)	(0/0/6/62)
	ventral (0/1/2/3)	(0/0/0/0)	(0/1/12/55)
Intercostal 5	dorsal (0/1/2/3)	(0/1/3/0)	(0/0/3/61)
	ventral (0/1/2/3)	(0/6/2/0)	(0/0/4/56)
Intercostal 6	dorsal (0/1/2/3)	(0/0/0/0)	(0/0/4/64)
	ventral (0/1/2/3)	(0/0/0/0)	(0/0/5/63)
Total	dorsal and ventral (0/1/2/3)	(0/7/5/0)	(0/1/64/467)

87.8%.

The median lung sliding scores at observed sites without adhesions were: 3.0 at the third intercostal space; 3.0 at the fourth intercostal space; 3.0 at the fifth intercostal space; 3.0 at the sixth intercostal space; 3.0 at the dorsal side; and 3.0 at the ventral side.

Discussion

In the present study, a high-frequency linear probe was selected for the visualization of the pleural line. By angling the reference mark of the probe slightly in the dorsocaudal direction rather than straight in the caudal direction, it was easy to visualize the pleural line at the third intercostal space of the anterior chest area. Moreover, expert skills were not required for the detection of pleural line movement, this examination can be easily accomplished in a typical operating room with equipment for respiratory management with forced ventilation. The operability was straightforward, and the examination itself was simple.

With pleural adhesions, the lung sliding score on lung ultrasound decreased significantly ($P<0.0001$), with sensitivity of 100% and specificity of 87.8%. These results can be explained in the following manner. “Lung sliding,” a term coined by Lichtenstein et al., is observed on ultrasound as the movement of parietal pleura and visceral pleura that occurs with respiratory motion (81). Lung sliding could be clearly observed at sites with active pleural sliding movements that occur with respiration, and lung sliding decreased where pleural movement was not active, even at normal sites without adhesions. The author initially postulated that decreased lung sliding would be observed more on the cranial side than on the caudal side and on the dorsal side more

than on the ventral side based on the anatomical structure of the lung. However, every median lung sliding score was 3.0 for the third through sixth intercostal spaces and for both dorsal and ventral sides. This may have occurred because “the area percentage of the observed site in which lung sliding was observed” rather than “how many centimeters the observed site shifted in the cranio-caudal direction” was evaluated. In other words, if at least 80% of the area within the observed site moved, then the lung sliding score would be 3, regardless of actual displacement distance. There is a specific reason why the lung sliding scores were classified by percentage of movement area that moved rather than by the movement distance. Indeed, there is a report that measured the distance of lung sliding movement in chest ultrasound examination of pleural adhesions in humans (76). However, unlike humans, dogs vary greatly in size depending on the breed, from small dogs such as Chihuahuas to large dogs such as Great Danes. Beagles generally have a uniform body size, and their individual differences can be negligible. However, considering the clinical application of the present examination method in the future, using a classification by the percentage of area that moved rather than by the distance of movement would be more practical and appropriate. Based on the above, the above-mentioned ultrasound method should be combined with other tests to make a definitive diagnosis of the presence of canine pleural adhesions.

Because only healthy dogs were tested in a specific breed, future investigations should be conducted tests in other breeds and clinical cases. However, this method appears to be a highly reliable tool for excluding canine pleural adhesions.

Ultrasound detection of pleural adhesions may be more useful in dogs than in humans. For detecting pleural adhesions using lung ultrasound in humans, the sensitivity and specificity were reported to be: 63.6% and 79.4% at the upper thoracic area and 81.5% and 81.0% at the lower thoracic area (56); 80.6% and 96.1% (78), respectively; and 88.0% and 82.6% (79), respectively. Pleural adhesion examination with lung ultrasound in dogs in the present examination resulted in a sensitivity of 100% and specificity of 87.8%, indicating a greater sensitivity and similar specificity compared to the reports in humans. All pleural adhesions in the present study developed at the fifth intercostal space along the thoracic wall incision line. The lateral thoracic wall at the fifth intercostal space is flat, allowing a relatively easy visualization of the lungs on ultrasound, and lung sliding can be examined clearly even in normal lungs at this site. This may explain the reasons why favorable results were obtained in the present examination. Pleural adhesions caused by surgical damage appear at the incision line or the surgically injured site. For example, they occur between the pericardium and pleura in surgeries that entail pericardial resection. In the present study, they appeared

between the lung (visceral pleura) and the thoracic wall (parietal pleura) at the fifth intercostal space. Pleural adhesions caused by endogenous factors, such as lung cancer or abscess, develop at these regions. In other words, for future clinical application of the present examination method, it is necessary to verify its sensitivity and specificity in detecting pleural adhesions at sites other than the fifth intercostal space. In addition, it has been reported in humans that lung ultrasound sensitivity is lower in the upper lung region than in the lower lung region (56). Thus, it is also necessary for dogs to determine whether there are differences between the cranial and caudal sides in the sensitivity for detecting pleural adhesions through lung sliding. Furthermore, it is essential to verify whether the present examination method can detect canine pleural adhesions in conditions such as obesity and emphysema that are known to hinder detection of lung sliding (56). In addition, assessment of lung sliding could judge only the presence or absence of pleural adhesion in this study. Further study is needed to make sure whether a decreased lung sliding score can detect partial pleural adhesions.

Conclusions

In conclusion, the present results showed that the examination of lung sliding by thoracic ultrasound has a high diagnostic value for detecting canine pleural adhesions and is useful in identifying adhesion sites before thoracic surgery. However, this result is limited to healthy dogs. Thus, information about the feasibility and accuracy of this technique in pathophysiological models needs to be obtained by further research.

Chapter 5

General Discussion

The objective in Chapter 2 was to elucidate the time-dependent degradation process in insoluble hyaluronic acid formulations with a controlled degradation rate. Sodium hyaluronate was treated with the conditions under which the treatment time was set to every 10 minutes from 0 to 90 minutes, and their IR and swelling rate were investigated subsequently. This study suggested that swelling ratio in control can be controlled by adjusting the treatment time, and the 1740 cm^{-1} absorption peak of IR is the predictable indicators of swelling rate. Three types of insoluble hyaluronic acid membrane with different swelling ratios (three for each type) were created for investigation of degradation process. The degradation score and swelling ratio showed a strong correlation between each other. Chapter 2 revealed one of controllable factor for swelling ratio of hyaluronic acid formulations. It also suggested that the correlations between IR absorption peak at 1740 cm^{-1} and swelling ratio and between IR absorption peak at 1740 cm^{-1} and degradation speed. In addition, it showed that the hyaluronic acid formulations is degraded gradually changes with time. Generated hyaluronic acid formulations had no byproducts through the generation process. The relationship of

insolubilization, swelling rate, and degradation start rate is inferred as follow. Functional group of hyaluronic acid was replaced -COONa to -COOH caused by treatment with acetic anhydride. Involving this change, intermolecular hydrogen bridge was formed and increased insolubilizing. According to reaction time with acetic anhydride, the replacement from -COONa to -COOH would be increased. When it was degraded, this reaction might be retrograded, and returned to the original -COONa to cleave hydrogen bond, then the membrane would probably swell. Therefor the control of reaction time might lead to degradation start rate.

In Chapter 3, the purpose is to test the effectiveness of insoluble hyaluronic acid membrane for postthoracotomy adhesion and operability. Using an insoluble hyaluronic acid membrane that remains in the surgical wound during the period when postoperative adhesions are formed and that has a swelling rate sufficient to maintain its shape as a physical barrier, the author tested the postoperative adhesion prevention effect and manipulability of the membrane. A previous report showed an effect of preventing post-thoracotomy adhesion using glycerin and surface water induction technology as a post-thoracic surgery adhesion prevention agent in dogs (25). Insoluble hyaluronic acid membranes are not damaged with normal handling but are susceptible to tears, and once they are torn, the damage may progress. Although little concern was paid to

manipulability in general thoracotomy, its use in thoracoscopic surgery with a small incision wound of 3.0 to 6.0 cm has been increasing recently (66). This gives rise to more concern about the damage to insoluble hyaluronic acid membranes and reduced manipulability as they are introduced into the thoracic cavity through a small incision hole. Thus, the small size of the incisions used for VATS (3–6 cm) and the use of specialized instruments significantly differe from those used in regular thoracotomy. In Chapter 3, whether the test membrane could be easily used under the special conditions imposed by VATS was investigated, and the macroscopic and histopathological investigations of inflammatory and immunological reactions in VATS were conducted. About the operativity of this membrane, membrane insertion in all other animals in the experimental group was achieved successfully except for that in one animal, the membrane was torn into multiple pieces while delivering from the small ~3.5-cm incision for left-sided VATS to the thoracic cavity, making it difficult to cover the target site completely. There were no differences in operability with wet gloves or with a wet wound protector placed at the small incision site and the membrane did not hinder the chest closing procedure. In the experimental group, adhesions were observed between the chest wall and lungs in 2/5 animals, and blunt dissection of the adhesions was difficult to achieve in the exceptimal animal. Pulmonary interlobular adhesions were

few and the median adhesion score was 0. In the control group, adhesions were observed in all animals, and the median adhesion score was 2.5. In the macroscopic examination at sacrifice, there were no inflammatory responses in the thoracic cavity in the experimental group. Histopathological analysis also showed no apparent induction of inflammatory changes or any foreign body reaction. This result suggests that the test membrane dissolves spontaneously within the thoracic cavity and can be absorbed into the body which does neither remain as a foreign substance nor cause any inflammatory response or foreign body reaction. The issue of this study was surgical invasiveness because only wedge resection of the lung lobe was performed using an automatic suture device in this study. However, the test membrane used in this study showed satisfactory operability in VATS. Following are possible reasons for high postoperative adhesion prevention effect obtained with insoluble hyaluronic acid membranes. First is that insoluble hyaluronic acid functions as a superior physical barrier. As shown in Chapter 2, this may be due to the fact that control of the degree of insolubility of hyaluronic acid leads to control of the swelling rate, suggesting the creation of an insoluble hyaluronic acid membrane with a low swelling rate allows it to function as a physical barrier for the necessary postoperative duration. The second reason may be the high water-retaining capacity of hyaluronic acid. When hyaluronic acid is hydrolyzed in the

body, a large amount of water accumulates in the surrounding area. It is also possible that the membrane simultaneously dilutes inflammatory substances produced during inflammation. In fact, retention of pleural fluid was seen together with liquefied test membranes during autopsy in one of my experimental group in which insoluble hyaluronic acid membranes had been introduced. The high biocompatibility and safety of hyaluronic acid may also have postoperative adhesion prevention effects. The response of hyaluronic acid *in vivo* differs depending on its molecular weight. Low molecular weight hyaluronic acid acts toward the induction of inflammation such as lymphocyte rolling via CD44 during inflammation (82), whereas high molecular weight hyaluronic acid shows anti-inflammatory activity within the body (83, 84). The insoluble hyaluronic acid membrane used as the test membrane in this study has a high molecular weight, and so may have acted toward the inhibition of inflammation(49). In this Chapter 3, one of limitations is less invasive than clinical cases. Therefore, in future investigations, induction of adhesions will need to be compared between use and non-use of the test membrane in surgeries with a greater degree of invasiveness, such as lobectomy or pericardial incision, instead of wedge resection.

The objective in Chapter 4 is to confirm whether postoperative adhesions can be detected, in case the adhesions cannot be prevented completely. Noninvasive methods

of detecting postthoracotomy adhesions in dogs were performed using ultrasonography of the lung sliding. The median lung sliding score of the 12 sites that showed pleural adhesions was 1.5. The median lung sliding score of the 521 sites that did not show pleural adhesions was 3.0. The lung sliding score was significantly decreased in the presence of adhesions. The sites with pleural adhesions observed with thoracotomy coincided with the sites with decreased lung sliding scores on lung ultrasound. The ultrasound examination detected pleural adhesions with a sensitivity of 100.0% and a specificity of 87.7%. These results showed that the examination of lung sliding by thoracic ultrasound has a high diagnostic value for detecting canine pleural adhesions and is useful in identifying adhesion sites before thoracic surgery.

From the aforementioned series of studies, the present study suggests that the following conclusions could be made in regard to the application of insoluble hyaluronic acid and its preparations. First, the present study clarified a part of the controlling factors of the decomposition rate of hyaluronic acid, and also clarified its decomposition process which have not been elucidated so far. It implies that swelling rate of the hyaluronic acid preparation can be controlled by changing the -COONa/-COOH ratio by changing the insolubilization process duration. Furthermore, it was possible to manipulate the decomposition starting time in simulated body fluids

by controlling this swelling ratio. Hyaluronic acid used in medicine has various requirements such as hardness, viscosity and duration of effect. The hyaluronic acid preparation currently being used *in vivo* primarily manipulates the molecular weight to control the duration of effect *in vivo* (38). Application of the results of the present study not only opens the way to develop new processing methods for hyaluronic acid preparations, but also creating a variety of hyaluronic acid preparations that have never been done. Moreover, by clarifying the required swelling ratio of insoluble hyaluronic acid for creating the post-operative adhesion inhibitor, it can not only be used for post-thoracotomy adhesion, but also can be expected to be applicable for other diseases including joint contracture, via the high adhesion prevention effect.

Furthermore, the fact that high post-operative adhesion prevention effect was shown in a dog open thoracotomy model may change the history of thoracic surgery. The worsening of operability and visual clarity during surgery and increase in bleeding due to tissue adhesion during a second-time thoracotomy is a post-operative complication well known to that all thoracic surgeons. If an operation field similar to the initial surgery can be obtained for the re-operation without causing complications, it is possible to reduce the burden on the patients and the fatigue of surgeons, thereby shortening the hospitalization period and reducing the cost. This is a major benefit for

both patients and surgeons. In addition, the fact that the membrane shown to be effective in operability is not limited to regular thoracotomy, it can also be applied to a special surgical method like VATS that is ensured for future development, shows its promising contribution to the development of thoracic surgery. In fact, this is an extremely unique post-operative adhesion inhibitor that is comprised of pure hyaluronic acid without any impurities, as described in Chapter 2, and is different from conventional adhesion inhibitors that is primarily comprised of substances that do not exist *in vivo* (21, 22), and post-operative adhesion inhibitors that are primarily comprised of carboxymethyl-cellulose (12, 13) which that are currently frequently used for the abdominal area. The fact that the membrane is consisted only of hyaluronic acid, which is present in the body and biodegradable, showed a high postoperative adhesion prevention effect makes it different from conventional adhesion inhibitors, especially from the viewpoint of safety in clinical application.

Furthermore, being able to demonstrate a non-invasive detection method of pleurodesis in dogs in an actual open thoracotomy case for the first time in the world is significally meaningful. Although some veterinarians may be able to detect the loss of respiratory activity in a lung due to adhesion in the chest area based on one's own experience and knowledge, the present study provided a method that can detect

pleurodesis on the basis of measurement data, instead of empirical rule. Moreover, the present study suggested that by making a criterion based on the ratio of lung movement rather than the ratio of the distance the lung moved like in humans, it suggested a method that can be used regardless of the body type or the dog’s breed. Furthermore, ultrasonic examinations in a recumbent position can be performed even on a dog under a poor respiratory condition, and, dogs may be inspected under the owner's attendance or oxygen mask, depending on the condition. Compared with CT examination that requires isolation under general anesthesia, the physical and psychological burden of the patient is greatly reduced. This detection method not only makes it easy to plan a dog's chest re-operation but can also be used for daily examinations due to its non-invasiveness and simplicity. A future task of this study, it is essential to verify whether the present examination method can detect canine pleural adhesions in clinical cases such as obesity and emphysema that are known to hinder detection of lung sliding.

However, the present study has enabled a new step forward advancing medicine through the development of a *de novo* hyaluronic acid preparation, and provides a possibility for a new treatment option for not only thoracic surgery in humans and dogs but also in other surgical fields, as well as advancing thoracic surgery and examination of dogs.

Conclusions

This study elucidated the following points. First, part of the degradation process of a hyaluronic acid formulation, which has long remained unclear, was elucidated. The swelling rate is controlled by making the formulation insoluble, and the degradation rate of hyaluronic acid formulation can be controlled by adjusting the swelling rate. This discovery has the potential to change the flow of future developments in hyaluronic acid formulations. This is because hyaluronic acid formulations, which have no potentially harmful byproducts and for which the residual period in the body can be controlled, are effective in preventing post-thoracic surgery adhesions, as well as having other potential clinical applications. For example, they are promising for clinical applications to prevent joint contracture by introduction into the joint.

Next, post-thoracic surgery adhesions could be prevented at a high rate in dogs with test membranes that used a hyaluronic acid formulation in which the degradation rate was adjusted. With this method of preventing post-thoracic surgery adhesions, no problems were encountered even when the gloves or equipment were wet. Moreover, even thoracoscopic surgery with small incision wounds could be performed without loss of manipulability. Compared with the carboxymethyl cellulose membranes currently in

wide use as agents for preventing post-abdominal surgery adhesion, hyaluronic acid membranes are considered to have superior aspects including both the post-thoracic surgery adhesion prevention effect and also manipulability. Moreover, if they are useful as a post-thoracic surgery adhesion prevention agent, they will be also obviously promising for use as a post-abdominal surgery adhesion prevention agent.

This study also suggests that the adhesion sites can be detected noninvasively when pleural adhesions have developed. In particular, the finding that the presence of lung sliding indicates the absence of adhesions at that site is very significant for determining the operative procedure before thoracic surgery. These findings are useful not only in examining the effectiveness of the test membrane, but also in procedures such as determining the incision site in dogs with a history of thoracic surgery or the technique for thoracic surgery in dogs with thoracic tumors or other conditions for which there is concern regarding thoracic adhesions, even without a history of thoracotomy.

The results of this study make it possible to predict the degradation rate of insoluble hyaluronic acid formulations by controlling the swelling rate during preparation. The use of insoluble hyaluronic acid formulations will help to prevent the blood loss, time loss, and poor visual field that occur with separation of adhering

pulmonary lobes from the thoracic wall during repeat thoracotomies.

The results obstained in this study will also allow the noninvasive, accurate prediction of the status of adhesions within the thoracic cavity before visual confirmation. In addition to its use as a post-thoracic surgery adhesion prevention agent, novel approaches to clinical applications of hyaluronic acid formulations will also become possible. These results may contribute to many areas of medicine over a broad range, not limited to thoracic surgery.

References

1. Hong G, Vilz TO, Kalff JC, Wehner S. [Peritoneal adhesion formation]. Chirurg. 2015;86(2):175-80.

2. ten Broek RP, Issa Y, van Santbrink EJ, Bouvy ND, Kruitwagen RF, Jeekel J, et al. Burden of adhesions in abdominal and pelvic surgery: systematic review and met-analysis. BMJ. 2013;347:f5588.

3. Muschalla F, Schwarz J, Bittner R. Effectivity of laparoscopic inguinal hernia repair (TAPP) in daily clinical practice: early and long-term result. Surg Endosc. 2016;30(11):4985-94.

4. Alizzi AM, Summers P, Boon VH, Tantiongco JP, Thompson T, Leslie BJ, et al. Reduction of post-surgical pericardial adhesions using a pig model. Heart Lung Circ. 2012;21(1):22-9.

5. Oizumi H, Naruke T, Watanabe H, Sano T, Kondo H, Goya T, et al. [Completion pneumonectomy--a review of 29 cases]. Nihon Kyobu Geka Gakkai Zasshi. 1990;38(1):72-7.

6. Yim AP, Liu HP, Hazelrigg SR, Izzat MB, Fung AL, Boley TM, et al. Thoracoscopic operations on reoperated chests. Ann Thorac Surg. 1998;65(2):328-30.

7. Getman V, Devyatko E, Wolner E, Aharinejad S, Mueller MR. Fleece bound

sealing prevents pleural adhesions. Interact Cardiovasc Thorac Surg. 2006;5(3):243-6.

8. Loop FD. Catastrophic hemorrhage during sternal reentry. Ann Thorac Surg. 1984;37(4):271-2.

9. Braxton JH, Higgins RS, Schwann TA, Sanchez JA, Dewar ML, Kopf GS, et al. Reoperative mitral valve surgery via right thoracotomy: decreased blood loss and improved hemodynamics. J Heart Valve Dis. 1996;5(2):169-73.

10. Diamond MP, Burns EL, Accomando B, Mian S, Holmdahl L. Seprafilm(R) adhesion barrier: (1) a review of preclinical, animal, and human investigational studies. Gynecol Surg. 2012;9(3):237-45.

11. Diamond MP, Burns EL, Accomando B, Mian S, Holmdahl L. Seprafilm((R)) adhesion barrier: (2) a review of the clinical literature on intraabdominal use. Gynecol Surg. 2012;9(3):247-57.

12. Ozerhan IH, Urkan M, Meral UM, Unlu A, Ersoz N, Demirag F, et al. Comparison of the effects of Mitomycin-C and sodium hyaluronate/carboxymethylcellulose [NH/CMC] (Seprafilm) on abdominal adhesions. Springerplus. 2016;5(1):846.

13. Osawa H, Nishimura J, Hiraki M, Takahashi H, Haraguchi N, Hata T, et al. Regeneration of peritoneal mesothelial cells after placement of hyaluronate

carboxymethyl-cellulose (Seprafilm(R)). Surg Today. 2017;47(1):130-6.

14. Lefort B, El Arid JM, Bouquiaux AL, Soule N, Chantreuil J, Tavernier E, et al. Is Seprafilm valuable in infant cardiac redo procedures? J Cardiothorac Surg. 2015;10:47.

15. Buyukkale S, Citak N, Isgorucu O, Sayar A. A bioabsorbable membrane (Seprafilm(R)) may prevent postoperative mediastinal adhesions following mediastinoscopy: an experimental study in rats. Int J Clin Exp Med. 2015;8(7):11544-8.

16. Sumi Y, Yamashita K, Kanemitsu K, Yamamoto M, Kanaji S, Imanishi T, et al. Simple and Easy Technique for the Placement of Seprafilm During Laparoscopic Surgery. Indian J Surg. 2015;77(Suppl 3):1462-5.

17. Koketsu S, Sameshima S, Okuyama T, Yamagata Y, Takeshita E, Tagaya N, et al. An effective new method for the placement of an anti-adhesion barrier film using an introducer in laparoscopic surgery. Tech Coloproctol. 2015;19(9):551-3.

18. Tsuruta A, Itoh T, Hirai T, Nakamura M. Multi-layered intra-abdominal adhesion prophylaxis following laparoscopic colorectal surgery. Surgical endoscopy. 2015;29(6):1400-5.

19. Altuntas YE, Kement M, Oncel M, Sahip Y, Kaptanoglu L. The effectiveness of hyaluronan-carboxymethylcellulose membrane in different severity of adhesions

observed at the time of relaparotomies: an experimental study on mice. Dis Colon Rectum. 2008;51(10):1562-5.

20. Kusuki I, Suganuma I, Ito F, Akiyama M, Sasaki A, Yamanaka K, et al. Usefulness of moistening seprafilm before use in laparoscopic surgery. Surg Laparosc Endosc Percutan Tech. 2014;24(1):e13-5.

21. Takagi K, Tsuchiya T, Araki M, Yamasaki N, Nagayasu T, Hyon SH, et al. Novel biodegradable powder for preventing postoperative pleural adhesion. J Surg Res. 2013;179(1):e13-9.

22. Izumi Y, Takahashi Y, Kohno M, Nomori H. Cross-linked poly(gamma-glutamic acid) attenuates pleural and chest wall adhesions in a mouse thoracotomy model. Eur Surg Res. 2012;48(2):93-8.

23. Karacam V, Onen A, Sanli A, Gurel D, Kargi A, Karapolat S, et al. Prevention of pleural adhesions using a membrane containing polyethylene glycol in rats. Int J Med Sci. 2011;8(5):380-6.

24. Akerberg D, Posaric-Bauden M, Isaksson K, Andersson R, Tingstedt B. Prevention of pleural adhesions by bioactive polypeptides - a pilot study. Int J Med Sci. 2013;10(12):1720-6.

25. Noishiki Y, Shintani N. Anti-adhesive membrane for pleural cavity. Artif

Organs. 2010;34(3):224-9.

26. Janosi A, Vass A, Benedek S. [Intravascular hemolysis caused by intravenous glycerin infusion in a patient with artificial mitral valve]. Orv Hetil. 1995;136(20):1055-7.

27. Murakami S, Yasuda T, Kushikata T, Hashimoto H, Hirota K. [Case of hemoglobinuria following glycerin enema]. Masui. 2007;56(6):689-91.

28. Meyer K, Palmer J, Palmer J, Meyer L. The polysaccharide of the vitreous humor. J Biol Chem. 1934;107:629-34.

29. Zako M, Iwaki M, Yoneda M, Miyaishi O, Zhao J, Suzuki Y, et al. Molecular cloning and characterization of chick sialoprotein associated with cones and rods, a developmentally regulated glycoprotein of interphotoreceptor matrix. J Biol Chem. 2002;277(28):25592-600.

30. Lebl MD, Martins JR, Nader HB, Simoes Mde J, De Biase N. Concentration and distribution of hyaluronic acid in human vocal folds. Laryngoscope. 2007;117(4):595-9.

31. Kim YS, Park JY, Lee CS, Lee SJ. Does hyaluronate injection work in shoulder disease in early stage? A multicenter, randomized, single blind and open comparative clinical study. J Shoulder Elbow Surg. 2012;21(6):722-7.

32. Takahashi K, Hashimoto S, Kurosaki H, Kato K, Majima T, Shindo Y, et al. A pilot study comparing the efficacy of radiofrequency and microwave diathermy in combination with intra-articular injection of hyaluronic acid in knee osteoarthritis. J Phys Ther Sci. 2016;28(2):525-9.

33. Estades-Rubio FJ, Reyes-Martin A, Morales-Marcos V, Garcia-Piriz M, Garcia-Vera JJ, Peran M, et al. Knee Viscosupplementation: Cost-Effectiveness Analysis between Stabilized Hyaluronic Acid in a Single Injection versus Five Injections of Standard Hyaluronic Acid. Int J Mol Sci. 2017;18(3):658.

34. Chen TA, Yeh CY. Long-term Follow-up of Adhesion Prevention With Use of Hyaluronic Acid-carboxymethylcellulose Membrane (Seprafilm). Ann Surg. 2017;265(4):e27.

35. Takeuchi H, Kitade M, Kikuchi I, Shimanuki H, Kinoshita K. A novel instrument and technique for using Seprafilm hyaluronic acid/carboxymethylcellulose membrane during laparoscopic myomectomy. J Laparoendosc Adv Surg Tech A. 2006;16(5):497-502.

36. Thareja SK, Sadhwani D, Alan Fenske N. En coup de sabre morphea treated with hyaluronic acid filler. Report of a case and review of the literature. Int J Dermatol. 2015;54(7):823-6.

37. Talarico S, Meski AP, Buratini L, Manela-Azulay M, Simpson H, Sidou F, et al. High Patient Satisfaction of a Hyaluronic Acid Filler Producing Enduring Full-Facial Volume Restoration: An 18-Month Open Multicenter Study. Dermatol Surg. 2015;41(12):1361-9.

38. Ran W, Wang X, Hu Y, Gao S, Yang Y, Sun J, et al. [Crosslinking sodium hyaluronate gel with different ratio of molecular weight for subcutaneous injection: animal experimental study and clinical trials subcutaneous injection]. Zhonghua Zheng Xing Wai Ke Za Zhi. 2015;31(3):198-201.

39. Choi SC, Yoo MA, Lee SY, Lee HJ, Son DH, Jung J, et al. Modulation of biomechanical properties of hyaluronic acid hydrogels by crosslinking agents. J Biomed Mater Res A. 2015;103(9):3072-80.

40. Credi C, Biella S, De Marco C, Levi M, Suriano R, Turri S. Fine tuning and measurement of mechanical properties of crosslinked hyaluronic acid hydrogels as biomimetic scaffold coating in regenerative medicine. J Mech Behav Biomed Mater. 2014;29:309-16.

41. Y. Isono YN. Method for manufacturing water-insoluble molded article and water-insoluble molded article. International Patent. 2015:WO/2015/029892.

42. Atasay B, Erdeve O, Arsan S, Turmen T. Effect of sodium alginate on acid

gastroesophageal reflux disease in preterm infants: a pilot study. Journal of clinical pharmacology. 2010;50(11):1267-72.

43. Park S, Park KY, Yeo IK, Cho SY, Ah YC, Koh HJ, et al. Investigation of the degradation-retarding effect caused by the low swelling capacity of a novel hyaluronic Acid filler developed by solid-phase crosslinking technology. Ann Dermatol. 2014;26(3):357-62.

44. Jaklitsch MT, Mery CM, Lukanich JM, Richards WG, Bueno R, Swanson SJ, et al. Sequential thoracic metastasectomy prolongs survival by re-establishing local control within the chest. J Thorac Cardiovasc Surg. 2001;121(4):657-67.

45. Voltolini L, Paladini P, Luzzi L, Ghiribelli C, Di Bisceglie M, Gotti G. Iterative surgical resections for local recurrent and second primary bronchogenic carcinoma. Eur J Cardiothorac Surg. 2000;18(5):529-34.

46. Aziz TM, Saad RA, Glasser J, Jilaihawi AN, Prakash D. The management of second primary lung cancers. A single centre experience in 15 years. Eur J Cardiothorac Surg. 2002;21(3):527-33.

47. Alfieris GM, Swartz MF, Lehoux J, Bove EL. Long-Term Survival and Freedom From Reoperation After Placement of a Pulmonary Xenograft Valved Conduit. Ann Thorac Surg. 2016;102(2):602-7.

48. Alsoufi B, Fadel B, Bulbul Z, Al-Ahmadi M, Al-Fayyadh M, Kalloghlian A, et al. Cardiac reoperations following the Ross procedure in children: spectrum of surgery and reoperation results. Eur J Cardiothorac Surg. 2012;42(1):25-30; discussion -1.

49. van Goor H. Consequences and complications of peritoneal adhesions. Colorectal Dis. 2007;9 Suppl 2:25-34.

50. Bruggmann D, Tchartchian G, Wallwiener M, Munstedt K, Tinneberg HR, Hackethal A. Intra-abdominal adhesions: definition, origin, significance in surgical practice, and treatment options. Dtsch Arztebl Int. 2010;107(44):769-75.

51. Orton EC, Hackett TB, Mama K, Boon JA. Technique and outcome of mitral valve replacement in dogs. J Am Vet Med Assoc. 2005;226(9):1508-11, 0.

52. Ehrhart N, Ehrhart EJ, Willis J, Sisson D, Constable P, Greenfield C, et al. Analysis of factors affecting survival in dogs with aortic body tumors. Vet Surg. 2002;31(1):44-8.

53. Bleakley S, Duncan CG, Monnet E. Thoracoscopic Lung Lobectomy for Primary Lung Tumors in 13 Dogs. Vet Surg. 2015;44(8):1029-35.

54. Gicking J, Aumann M. Lung lobe torsion. Compend Contin Educ Vet. 2011;33(4):E4.

55. Jin KN, Sung YW, Oh SJ, Choi YR, Cho H, Choi JS, et al. Association between

Image Characteristics on Chest CT and Severe Pleural Adhesion during Lung Cancer Surgery. PLoS One. 2016;11(5):e0154694.

56. Sasaki M, Kawabe M, Hirai S, Yamada N, Morioka K, Ihaya A, et al. Preoperative detection of pleural adhesions by chest ultrasonography. Ann Thorac Surg. 2005;80(2):439-42.

57. Y. Isono YN. Method for manufacturing water-insoluble molded article and water-insoluble molded article. Patent. 2015:WO/2015/029892,.

58. Haxaire K, Marechal Y, Milas M, Rinaudo M. Hydration of polysaccharide hyaluronan observed by IR spectrometry. I. Preliminary experiments and band assignments. Biopolymers. 2003;72(1):10-20.

59. Goodman GJ. An interesting reaction to a high- and low-molecular weight combination hyaluronic acid. Dermatol Surg. 2015;41 Suppl 1:S164-6.

60. Gold MH. Use of hyaluronic acid fillers for the treatment of the aging face. Clin Interv Aging. 2007;2(3):369-76.

61. Reichenbach S, Blank S, Rutjes AW, Shang A, King EA, Dieppe PA, et al. Hylan versus hyaluronic acid for osteoarthritis of the knee: a systematic review and meta-analysis. Arthritis Rheum. 2007;57(8):1410-8.

62. Foureman P, Mason JM, Valencia R, Zimmering S. Chemical mutagenesis

testing in Drosophila. IX. Results of 50 coded compounds tested for the National Toxicology Program. Environ Mol Mutagen. 1994;23(1):51-63.

63. Spencer MK, Radzinski NP, Tripathi S, Chowdhury S, Herrin RP, Chandran NN, et al. Pronounced toxicity differences between homobifunctional protein cross-linkers and analogous monofunctional electrophiles. Chem Res Toxicol. 2013;26(11):1720-9.

64. Uemura A, Nakata M, Goya S, Fukayama T, Tanaka R. Effective new membrane for preventing postthoracotomy pleural adhesion by surface water induction technology. Plos One. 2017;12(6):e0179815.

65. Uemura A, Fukayama T, Tanaka T, Baba Y, Shibutani M, Tanaka R. Development of an Anti-Adhesive Membrane for Use in Video-Assisted Thoracic Surgery. Int J Med Sci. 2018;15(7):689-95.

66. Carrott PW, Jr., Jones DR. Teaching video-assisted thoracic surgery (VATS) lobectomy. J Thorac Dis. 2013;5 Suppl 3:S207-11.

67. Karkhanis VS, Joshi JM. Pleural effusion: diagnosis, treatment, and management. Open Access Emerg Med. 2012;4:31-52.

68. Na MJ. Diagnostic tools of pleural effusion. Tuberc Respir Dis (Seoul). 2014;76(5):199-210.

69. Yu H. Management of pleural effusion, empyema, and lung abscess. Semin Intervent Radiol. 2011;28(1):75-86.

70. Gualdi GF, Volpe A, Polettini E, Jula GF. [Computed tomography and magnetic resonance in the TNM staging of pulmonary carcinoma]. Clin Ter. 1992;141(12):493-8.

71. Suzuki T. [Bacterial infections of the lung in the elderly]. Kyobu Geka. 2005;58(8 Suppl):714-7.

72. Satoh H, Kurishima K, Kagohashi K. Pneumothorax with postoperative complicated pleural adhesion. Tuberk Toraks. 2013;61(4):357-9.

73. Case JB, Mayhew PD, Singh A. Evaluation of Video-Assisted Thoracic Surgery for Treatment of Spontaneous Pneumothorax and Pulmonary Bullae in Dogs. Vet Surg. 2015;44 Suppl 1:31-8.

74. Shamir S, Mayhew PD, Zwingenberger A, Johnson LR. Treatment of intrathoracic grass awn migration with video-assisted thoracic surgery in two dogs. J Am Vet Med Assoc. 2016;249(2):214-20.

75. Mayhew P, Fransson B. Small Animal Laparoscopy and Thoracoscopy (AVS Advances in Veterinary Surgery). 2015.

76. Boos J, Fang J, Heidinger BH, Raptopoulos V, Brook OR. Dual energy CT angiography: pros and cons of dual-energy metal artifact reduction algorithm in patients

after endovascular aortic repair. Abdom Radiol (NY). 2017;42(3):749-58.

77. Elagha AA, Weissman G. Pacemaker Malfunction Attributed to Multidetector Cardiac Computed Tomography. Circulation. 2016;133(3):342-3.

78. Cassanelli N, Caroli G, Dolci G, Dell'Amore A, Luciano G, Bini A, et al. Accuracy of transthoracic ultrasound for the detection of pleural adhesions. Eur J Cardiothorac Surg. 2012;42(5):813-8; discussion 8.

79. Wei B, Wang T, Jiang F, Wang H. Use of transthoracic ultrasound to predict pleural adhesions: a prospective blinded study. Thorac Cardiovasc Surg. 2012;60(2):101-4.

80. Lisciandro GR. Abdominal and thoracic focused assessment with sonography for trauma, triage, and monitoring in small animals. J Vet Emerg Crit Care (San Antonio). 2011;21(2):104-22.

81. Lichtenstein DA, Menu Y. A bedside ultrasound sign ruling out pneumothorax in the critically ill. Lung sliding. Chest. 1995;108(5):1345-8.

82. Rios de la Rosa JM, Tirella A, Gennari A, Stratford IJ, Tirelli N. The CD44-Mediated Uptake of Hyaluronic Acid-Based Carriers in Macrophages. Adv Healthc Mater. 2017;6(4).

83. Gigis I, Fotiadis E, Nenopoulos A, Tsitas K, Hatzokos I. Comparison of two

different molecular weight intra-articular injections of hyaluronic acid for the treatment of knee osteoarthritis. Hippokratia. 2016;20(1):26-31.

84. Caires R, Luis E, Taberner FJ, Fernandez-Ballester G, Ferrer-Montiel A, Balazs EA, et al. Hyaluronan modulates TRPV1 channel opening, reducing peripheral nociceptor activity and pain. Nat Commun. 2015;6:8095.

Acknowledgement

My heartfelt appreciation goes to Prof. T. Nakajima-Kambe whose comments and suggestions were of inestimable value for my doctoral dissertations.

I am grateful acknowledge the supervising to Prof. K. Nakamura, Prof. P.C. Wang and Prof. Y. Ito for helpful discussions.

I express my sincere thanks to Associate Prof. R. Tanaka for his leadership and valuable comments.

My sincere thanks to Prof. Y. Noishiki and Prof. M. Shibutani for their useful advice.

I am grateful for the samples of new membrane provided by Mr. H. Ito, Mr. Y. Aso, Mr. S. Ogawa, Mr. T. Hayashi from Dainichiseika Color & Chemicals Mfg. Co., Ltd. (Tokyo, Japan) for use in this research.

This research was carried out as a collaborative development project contracted by the Japan Science and Technology Agency as recommissioned research for a membrane using surface water induction technology to prevent pleural adhesions. This research was funded by grants from the Japan Science and Technology Agency.

I would also like to express my gratitude to my family for their moral support and warm encouragement.

I appreciate all the people who have supported me.

要　旨

胸部術後癒着防止剤に対する需要は高く、現在も数多く研究されているが、未だ開発途上である。グリセリンを保水剤とした表層水誘導技術の先行研究において、高い胸部術後癒着防止効果が報告されている。ところがグリセリンは安全性に対する懸念があるため、より安全性の高いヒアルロン酸を保水剤として、同技術を用いた胸部術後癒着防止剤の開発を行うこととした。

術後癒着防止剤は癒着が形成される術後約 1 週間、分解されることなく切開部に留まる必要性がある。ところが、ヒアルロン酸製剤の分解速度制御因子と分解過程は未解明の部分が多かった。そこで第 2 章では、新規不溶化ヒアルロン酸製剤である被験膜を用いて、その分解速度の制御因子および分解過程を明らかにすることを試みた。ヒアルロン酸ナトリウムを不溶化処理し、不溶化処理時間が異なる 3 タイプの被験膜を作製した後、それぞれの分子構造を FT-IR を用いて分析した。さらに、擬似体液中での被験膜の経時的な形状変化についてもスコアリングした。その結果、不溶化処理時間を変化させることで、被験膜の膨張率と分解開始時間を制御可能であることが判明した。さらに、その分解過程についても明らかにすることができた。

第 3 章では、被験膜による胸部術後癒着防止効果とその操作性、炎症性と異物反応について、近年その利用が拡大している胸腔鏡手術において検証した。被験膜は胸腔内に問題なく挿入可能であり、手袋が濡れていてもその操作性は変わらなかった。実験群の癒着スコア中央値は 0 であり、コントロール群の癒着スコア中央値は 2.5 であった。肉眼的所見では、実験群で炎症反応はみられず、病理組織学的にも被験膜に対する明らかな炎症反応、異物反応は認められなかった。正常犬の肺葉部分切除は、疾患を有する臨床症例と比較して侵襲が低いという課題はあるが、被験膜は胸腔鏡手術において有用であることが示唆され

た。

第 4 章では、胸部術後癒着の非侵襲的検出の可否を目的とした。犬で超音波装置を用い、Lung Sliding（LS）の観察による胸部術後癒着の非侵襲的な検出方法について検証した。胸膜癒着が存在する 12 ヶ所の LS スコアは 1.5 であり、胸膜癒着の存在しない 521 ヶ所の LS スコアは 3.0 であった。LS は癒着部位で顕著に減少しており、超音波検査後に開胸下で確認した胸膜癒着発生部位と LS スコア低下部位は一致していた。本検査法による胸膜癒着検出は、感度 100.0%、特異度 87.7%であった。この結果から、本法は犬における胸膜癒着部位特定に有用であると考えられた。

本研究において、長らく未解明であったヒアルロン酸製剤の分解過程の一端を解明し、また、被験膜は犬の胸部術後癒着防止に有用であると考えられた。さらに、胸膜癒着発生時も、その非侵襲的検出が可能であると示唆された。これらから、胸部術後癒着防止剤としての有用な素材の開発とその有用性の非侵襲的検出方法確立にとどまらず、ヒアルロン酸製剤の臨床応用に対するこれまでにない利用方法の可能性を開拓できたと考えられる。

Abstract

There is a high demand for agents that prevent adhesions following thoracic surgery. While several studies of such agents are presently underway, they are still very much under development. A previous study found that surface water induction technology using glycerin as the humectant was highly effective for preventing postthoracotomy adhesions. However, as the safety of glycerin raises concerns, I decided to develop a postthoracotomy adhesion preventive agent using the same technology but with hyaluronic acid, a safer choice, for the humectant.

Postoperative adhesion preventive agents need to stay in the incision area without being dissolved for approximately one week postoperatively, which is the period when adhesions form. However, factors that control the degradation rate and process of hyaluronic acid are largely unknown. Therefore, in chapter 2, I attempted to elucidate factors that control the degradation rate and degradation process of hyaluronic acid using test membranes from a new insoluble hyaluronic acid preparation. Sodium hyaluronate was treated to become insoluble, and after preparing three types of test membranes with different insolubilization treatments, the molecular structure of each was analyzed using Fourier-transform infrared spectroscopy (FT-IR). Morphological changes over time of the test membranes in simulated body fluid were also scored. As a result, I found that the expansion rate of the test membrane and the time when it starts to degrade could be controlled by changing the insolubilization treatment duration. Furthermore, I was able to clarify the degradation process.

In chapter 3, I examined the postthoracotomy adhesion prevention effect and related operability of the test membranes, as well as inflammatory and foreign body reaction in thoracoscopic surgery, for which the test membrane has gained popularity in

recent years. The test membrane can be inserted into the pleural cavity without any problem, with no change to operability even if the surgeon's gloves become wet. The median score for adhesions was 0 in the experiment group, and 2.5 in the control group. Macroscopic findings revealed no inflammatory reaction in the experiment group. Histopathologically, there was no clear inflammatory reaction or any foreign body reaction to the test membranes. For partial lobectomy in normal dogs, minimal invasiveness is a challenge compared to in clinical cases with disease. My results suggested that the test membrane is useful for thoracoscopic surgery.

In chapter 4, I aimed to determine the advantages and disadvantages of non-invasive detection of postthoracotomy adhesions. I investigated a noninvasive method of detecting postthoracotomy adhesions by lung sliding (LS) observation using ultrasonography in dogs. The LS score of 12 sites with pleural adhesions was 1.5, and the LS score of 521 sites without pleural adhesions was 3.0. LS was remarkably reduced at adhesion sites, and the sites with pleural adhesion confirmed by thoracotomy after ultrasound examination were consistent with the sites with low LS scores. Pleural adhesion detection using the present test method had sensitivity of 100%, and specificity of 87.7%. Therefore, it appears that this method is useful for identifying pleural adhesion sites in dogs.

In the present study, I clarified one part of the degradation process of hyaluronic acid, which had long been unclear. I also found that the test membrane was useful for preventing postthoracotomy adhesions in dogs. Moreover, results suggested that even in the event of pleural adhesion onset, the adhesions can be detected non-invasively. Therefore, it appears that I developed a useful postthoractomy adhesion preventive agent that could aid in establishing an effective noninvasive method of detecting adhesions. My method could also open up novel methods of utilization of hyaluronic

acid preparations for clinical application.